Check for updates

Strategic design principles for greener biorefineries: a substrate–process matrix emphasizing complete lignocellulose utilization from various biomass feedstocks

Jianyu Guan,[†][a] Aamir Khan, [ID] [†][a] Yi Zhang,[b] Yixing Zhou,[b] Molly Meng-Jung Li, [ID] [b] Raffel Dharma Patria*[a] and Shao-Yuan Leu [ID] *[a,c,d,e]

Lignocellulosic biomass are promising feedstocks for sustainable biofuel and bioproduct production. Despite their abundance, however, only a fraction of biomass is utilized, highlighting their complex compositions and the need for advanced biorefinery technologies. This study investigates two biorefinery strategies, *i.e.*, pretreatment followed by catalytic transfer hydrogenolysis (PT-CTH) and reductive catalytic fractionation (RCF), aiming to harvest high-value lignin monomers from diverse biomass feedstocks including hardwood, softwood, grasses, barks, and seed coats. We classify these biomass feedstocks based on their lignin structures and physiochemical properties, which influence their reactivity and suitability for specific treatment processes. Through analyses on mass balance, environmental sustainability, and economic profitability, we propose recommendations and suggest future research directions to improve current processes for each biomass species. Our analysis reveals that while RCF converts lignin to higher monomer yields and exhibits higher economic feasibility, PT-CTH is more sustainable and utilizes the whole biomass more efficiently due to its efficient pretreatment. Hardwood and grass demonstrate high resource efficiency, with higher yields of monomers in RCF; softwood and barks are preferred feedstocks for PT due to higher extractive contents and carbohydrates compositions. Seed coats, rich in C-lignin, offer high potential for aromatic monomer production, but demonstrate lower resource efficiency while barks require tailored approaches due to their complex lignin units. This study proposes recommendations to advance efficient, sustainable biorefinery operations, exploiting the structural diversity of different biomass for optimized biomass utilization, and supports the development of more economical and environmentally friendly biorefinery techniques toward carbon neutrality.

Green foundation

1. The concept of "lignin-first" biorefinery techniques has recently been implemented to produce aromatic monomers, while the values of carbohydrates have been sometimes sacrificed. Here, we discuss the potential of building a bioeconomy with specific targets on carbohydrates the profitability and environmental protection.

2. Five major lignocellulosic biomass types are considered as feedstocks for two common thermochemical processes, namely, hardwood, softwood, grass, barks, and seed coats. We evaluate the potential values of each biomass in two major biorefinery approaches *via* their aromatic monomer yield and carbohydrates utilization efficiency.

3. Further studies on the development of greener biorefinery would rely on combining the benefits of low-temperature pretreatment, highly selective catalytic conversion processes, and advanced separation techniques, in order to treat more biomass in an integrated system.

[a]*Department of Civil and Environmental Engineering, The Hong Kong Polytechnic University, Hong Kong. E-mail: raffel-dharma.patria@connect.polyu.hk, syleu@polyu.edu.hk*

[b]*Department of Applied Physics, The Hong Kong Polytechnic University, Hong Kong*

[c]*Research Institute for Smart Energy (RISE), The Hong Kong Polytechnic University, Hong Kong*

[d]*Research Centre for Resources Engineering towards Carbon Neutrality (RCRE), The Hong Kong Polytechnic University, Hong Kong*

[e]*Research Institute of Future Food (RiFood), The Hong Kong Polytechnic University, Hong Kong*

†These authors have contributed equally to this work and are considered as first authors.

1. Introduction

Lignocellulosic biomass (LCB) is a promising resource for the sustainable production of biofuels and bioproducts, offering a potential solution to achieve carbon neutrality. Composed of cellulose, hemicellulose, and lignin, lignocellulosic biomass has long been utilized in the pulp and paper industry, where cellulose and hemicellulose are the primary components for utlization.[1] Based on the accumulated knowledge about cellulosic materials, many studies have been conducted to utilize

this biopolymer.[2] However, the low value and high energy content of lignin by-products derived from pulp mills have highlighted the need for more effective biorefinery technologies.[3] Overall, a total of 50 million tons of lignin are generated annually as a by-product.[4] Despite the annual production of 181.5 billion tons of lignocellulosic biomass, only 8.2 billion tons are currently utilized, underscoring the importance of advancing technologies to convert this abundant resource into useful products.[5]

Biorefining is an integrated process of various unit operations, aiming to maximize the potential of lignocellulosic biomass. Biorefinery techniques have been constructed on two major principles, *i.e.*, the sugar-based (biological) and syngas-based (thermochemical) platforms. The sugar-based platforms have focused on how to effectively hydrolyze cellulose and hemicellulose into sugars for fermentation to bioethanol and many other bio-products.[6] The syngas-based platforms, such as gasification and pyrolysis, have been designed for rapid production of syngas, bio-oil, and biochar from LCB.[7] Based on the two basic principles, the "lignin-first" concept has been introduced as an emerging approach for the valorization of lignin to produce high-value aromatic monomers for downstream applications, such as food, biopolymer, and pharmaceuticals.[8,9] This approach is crucial for balancing the low profitability of biorefinery practices that use non-food feedstock compared to conventional refineries and food-based biorefinery products. By doing so, it enhances the competitiveness of LCB in establishing a bio-economy.[10,11]

The high complexity of lignocellulosic biomass, however, presents significant technical challenges that must be addressed to fully realize the benefits of biorefinery technologies. Biomass consists of plant-based composite materials with physical and chemical properties that vary significantly from the harvesting plant species, parts, and conditions of the plants. This variability can lead to a wide range of products/by-products and yields in biorefining, impacting the economic viability of the selected techniques. As researchers and industries continue to explore innovative solutions, the effective utilization of lignin and the advancement of biorefinery technologies will be key to unlocking the full potential of lignocellulosic biomass. A comprehensive understanding of the relationship between biomass characteristics and processing methods is essential to fully clarify these benefits.

In this study, two lignin-first biorefinery processes were investigated, which are pretreatment followed by catalytic transfer hydrogenation (PT-CTH) and reductive catalytic fractionation (RCF) (Fig. 1). The two reaction routes have significantly different design principles and process conditions, while thermochemical catalytic hydrogenolysis is involved in both systems to depolymerize lignin into monomers.

PT-CTH and RCF are constructed based on different reaction principles, which offer distinct advantages for processing biomass. PT aims to fractionate lignocellulosic biomass into building block chemicals,[12] and CTH is included to depolymerize the fractionated lignin into monomers. RCF is a one-pot strategy which combines PT and CTH in one reactor.[13] Although some research works have tested and compared RCF's efficiency, only limited studies have addressed the issues of high temperature systems for carbohydrate utilization.[14–17]

We conducted a comprehensive data analysis on the PT-CTH and RCF processes applied to various biomass feedstocks suitable for biorefinery. Our analyses are presented in figures to highlight key insights, with detailed values provided in tables in the SI. Key parameters such as monomer yield, monomer selectivity (types of monomers produced), oligomer yield, and carbohydrate recovery were examined. Through mass balance analysis, we reviewed the product yields and resource efficiencies for each type of lignocellulosic biomass in both RCF and PT-CTH processes. We also explored the relationships between monomer yields and delignification, as well as monomer yield *versus* β-O-4 contents, across different studies involving RCF and PT-CTH for each biomass. Finally, we conducted preliminary quantification of environment
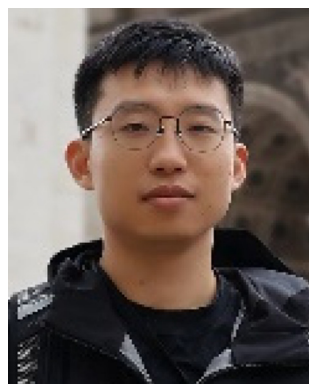
Jianyu Guan

Jianyu Guan is currently a PhD student at The Hong Kong Polytechnic University, under the supervision of Prof. Shao-Yuan (Ben) Leu, who leads the Green Energy Process Laboratory. His research focuses on biomass valorization, with particular interest in process control, biomass molecular architecture, and lignin depolymerization. He is particularly interested in applying solid-state NMR techniques to elucidate structural features of biomass that influence selective lignin separation and monomer production.

Aamir Khan

Aamir Khan received his BS degree in Environmental Engineering from the National University of Sciences and Technology, Pakistan, in 2014, conducting research on saline water treatment. He then earned his MS degree from the same university in 2019, conducting research on anaerobic wastewater treatment. Currently, he is doing his PhD at The Hong Kong Polytechnic University under the supervision of Professor Shao-Yuan Leu. His research focuses on the pretreatment and valorization of woody biomass into biofuels.
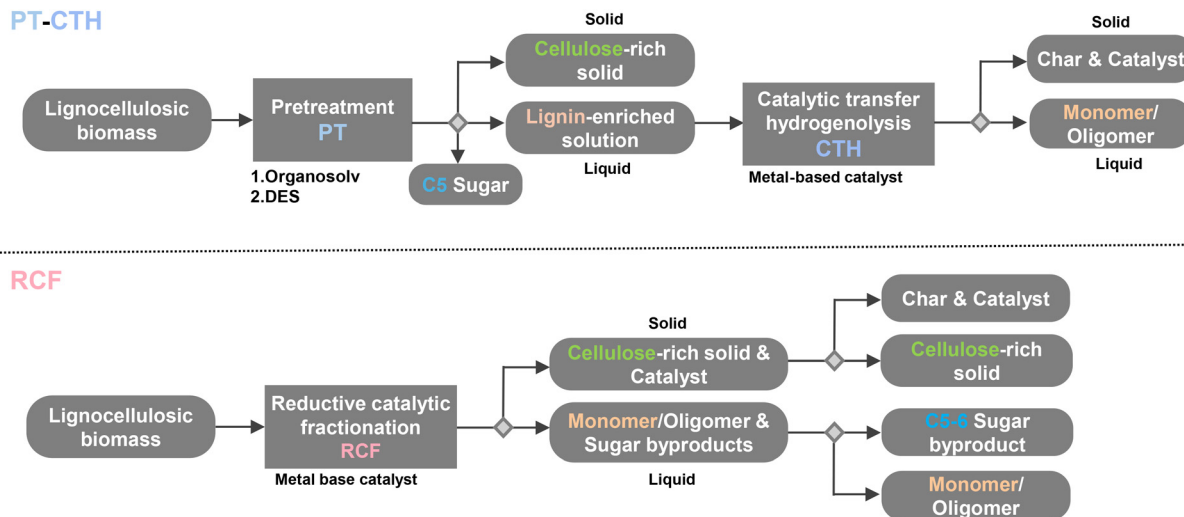
Fig. 1 Process flow of PT-CTH and RCF biorefinery processes. Color codes of the concerned processes and substrates used throughout this article: light blue: pretreatment followed by catalytic transfer hydrogenation (CTH); pink: reductive catalytic fractionation (RCF); green: cellulose; dark blue: mono sugar products; orange: lignin and its monomer product.

factors (E-factor), evaluated carbon sustainability based on energy consumption and biomass utilization, and quantified economic feasibility through cost–benefit analysis. Based on our findings, recommendations have been made to enhance current biorefinery techniques and directions for future research are suggested.

2. Classification of biomass

To better distinguish the impacts of verified biomass species on PT-CTH and RCF, lignocellulosic biomass feedstocks are first classified based on their physiochemical properties into five categories, which are (i) hardwood with guaiacol (G) and syringol (S) lignin, (ii) softwood with G lignin, (iii) grass (her-

baceous) with G, S, and hydroxycinnamate lignin, (iv) barks with suberin, and (v) seed coats with catechyl (C) lignin (Fig. 2). The unique lignin units and chemical composition of each biomass are listed in Table 1 and Fig. 3.[18–50]

2.1. Hardwood, softwood, and grass

Hardwood lignin is a promising candidate for the RCF process. In general, hardwood has both S-lignin and G-lignin with an S/G ratio ranging from 0.1 to 7.0 (Table 1). Despite having relatively low lignin content, hardwood lignin is characterized by a notably high proportion of β-O-4 linkages (55.6–99.1% of total lignin), indicating considerable potential for depolymerization. The hemicellulose in hardwood is primarily xylan, which is a C_5 sugar less desirable in the fermentation process. Softwood generally has higher lignin content
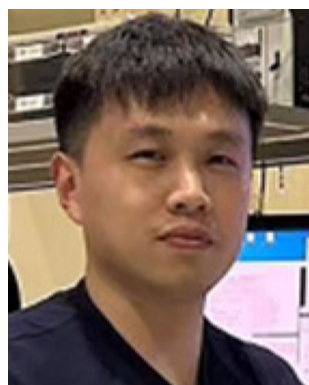
Yi Zhang is a postdoctoral fellow in the Applied Physics Department at The Hong Kong Polytechnic University. He obtained his PhD in Environmental Science and Engineering from Jiangsu University in 2023. His research focuses on the mechanisms and applications of photocatalysis/ photothermal catalysis in energy conversion. He is also interested in using synchrotron spectroscopic techniques to reveal the structural characteristics of heterogeneous catalysts.

Yi Zhang

Prof. Molly Meng-Jung Li is an Assistant Professor in the Applied Physics Department at The Hong Kong Polytechnic University. She completed her PhD in Inorganic Chemistry at the University of Oxford, for which she received a DPhil Swire Scholarship from University College. Her research focuses on nanomaterials and catalysis, particularly for hydrogen storage and production, fine chemicals, and environmental applications.

Molly Meng-Jung Li

She also specialises in synchrotron spectroscopic techniques to analyse nanocatalyst structures and reveal the origins of their performance in heterogeneous catalytic processes.
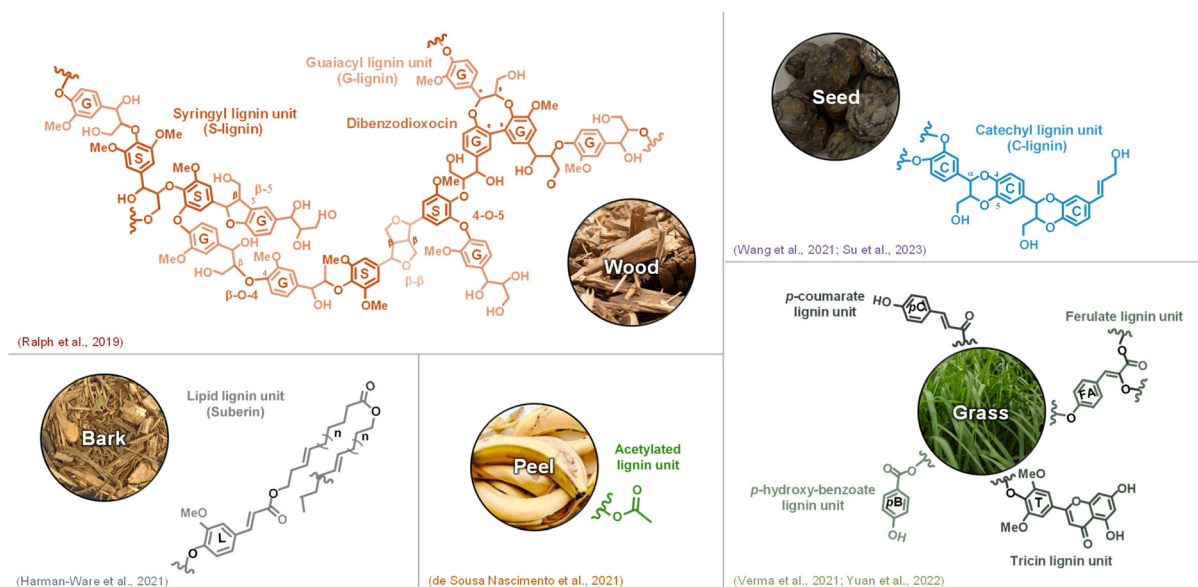
Fig. 2 Lignin model structures and unique lignin units investigated in this study.

than hardwood, ranging from 24.7% to 36.6%.[20,29,30] Unlike hardwood, softwood lignin is characterized by high G-lignin units with more side-chain structures and a lower proportion of β-O-4 linkages (31.2–38.1%). Consequently, direct RCF of softwood typically results in a higher production of oligomers and lower monomer yields (10–22%). However, the high proportion of G-units in softwood lignin (over 90%) allows for selective lignin depolymerization.[51] The dominant polysaccharide in softwood is mannose (about 12.1%), with xylan constituting only 6.2%.

Grass (herbaceous) biomass has significantly higher hemicellulose content (predominantly in the form of xylan) than woody biomass. Generally, grass also has higher ash content (5–10%), which can be incorporated into the lignin structure. In addition to G/S units, its lignin often contains unique aromatic end units, such as p-hydroxybenzoate-lignin, p-coumarate-lignin (pC), ferulate-lignin (F) and tricin-lignin.[51,53] This allows for the production of some specific monomers such as ethyl phenol and methyldihydroferulate (methyl-F). For more details on lignin units in hardwood, softwood, and grass, Lupoi *et al.* (2015) have provided extensive lists of β-O-4, resinol, phenyl-coumaran amounts of 30 plant samples and S/G ratios of 80 plant samples consisting of hardwood, softwood, and grass.[51]

Raffel Dharma Patria is a PhD student under the supervision of Prof. Shao-Yuan (Ben) Leu in The Hong Kong Polytechnic University. He received his BEng in chemical and biomolecular engineering from the Hong Kong University of Science and Technology in 2016 and obtained his MSc in chemical engineering from the University of California Berkeley in 2017. His research focuses on whole biomass utilization through pretreatment, enzymatic hydrolysis, fermentation, and catalytic transfer hydrogenolysis into aromatic monomers and biofuel.

Raffel Dharma Patria

Prof. Shao-Yuan (Ben) Leu is a licensed engineer of California (P.E.) and Hong Kong (HKIE). He has more than 15 years of experience in the research and development of innovative biorefinery technology to convert lignocellulosic biomass into biofuels and valuable products. At The Hong Kong Polytechnic University, Prof. Leu established the BioEnergy Laboratory aiming to forge biorefinery principles into practices. He has produced bioethanol, lactate, and 2,3-BDO and realized a novel diol-based organosolv pretreatment process in a pilot-scale vessel. Since 2013, Dr Leu has secured grants worth more than HK$42 million, published 110 peer-reviewed articles, filed 4 patents, and edited 1 book.

Shao-Yuan Leu

Table 1 S/G ratios or amount (wt% of biomass) of Klason lignin units in five biomass types

Biomass	Name	Klason lignin units[a]	Ref.
Hardwood	Poplar	S/G = 1.52–3.85	52
	Eucalyptus	S/G = 1.5–2.9	53
	Silver birch	S/G = 3.0–7.0	53
	European beech	S/G = 0.75	53
	Acacia	H : G : S = 1 : 1 : 0.1	53
	Cork oak	S/G = 1.2	53
	Teak	S/G = 0.7–0.8	53
Softwood	Maritime pine	S/G = 0.041	53
	Loblolly pine	H/G = 0.01	53
	Scotch pine	H/G = 0.048	53
	Pine	H : G : S = n.d. : 99 : 1	51
	Spruce	S/G = 0.0	51
Grass	Wheat straw	S : G : H : pCA : FA : T = 44 : 54 : 2 : 6 : 21 : 10	53 and 54
	Miscanthus	S : G : H : pCA : FA : T = 37 : 61 : 2 : 31.8 : 7.7 : 0	53 and 55
	Sorghum	S : G : H : pCA : FA : T = 32.7 : 63 : 4.3 : 50.9 : 6.3	56
	Rice straw	S : G : H : pCA : FA : T = 37.5 : 62.5 : 0 : n.d : n.d : n.d	51
	Bamboo	S : G : H : pCA : FA : T = 43 : 56.7 : 0 : 21.6 : 6.4 : 0.2	7
	Giant reed stalk	S : G : H : pCA : FA : T = 38.3 : 61.7 : n.d : n.d : n.d	53
	Corn cob	S : G : H : pCA : FA : T = 46 : 39 : 1 : 88.4 : 121 : 10.7	57
Barks	Monkeyhair tree (fossil)	Suberin = 26.3%	58
	European beech	Suberin = 48.3%	59
	Aspen	Suberin = 37.9%	59
	Sycamore maple	Suberin = 26.6%	59
	English oak	Suberin = 39.7%	59
	Evergreen oak	Suberin = 24.9%	59
	Cork oak	Suberin = 37.0–60.0%; S/G = 0.1	53 and 59
	Silver birch	Suberin = 32.2–58.6%; S/G = 0.1	53 and 59
	Canadian poplar	Suberin = 3.03%	59
	Willow	Suberin = 1.82%	59
	Maritime pine	Suberin = 1.5%	59
	Stone pine	Suberin = 2.5%	59
Seed coats (C-lignin)	Vanilla	Benzodioxane = 98%[b] of dimeric units *i.e.*, almost exclusively C-lignin	60
	Vanilla	C = 13%[c] wt-seed-coat	44
	Melocactus	Predominantly C-lignin	60
	Chinese tallow	C/(G + S) = 1.5[d]; C = 15.4%[c] wt-seed-coat	47
	Jatropha	C/(G + S) = 0.4[d]	48
	Candlenut	C/(G + S) = 0.7[d]	48
	Tung	C/(G + S) = 0.6[d]	48
	Castor	C/(G + S) = 4.2[d]	48
	Castor	C/(G + S) = 6.9[d]	61
	Castor	C = 4.6%[c] wt-seed-coat	62

[a] n.d. = not detected. [b] Measured by 2D NMR method. [c] Measured by ^{13}C NMR method. [d] Measured by thioacidolysis method.

2.2. Barks and seed coats

Barks and seed coats represent a frequently overlooked category of biomass, partly due to their low abundance when compared to hardwood, softwood, and grass. Research studies on RCF and PT-CTH of barks and seed coats are also more limited than those on hardwood, softwood, and grass. These residues typically have rapid growth cycles and contain relatively low cellulose content, but higher lignin content. The lignin content of these materials may be overestimated due to the presence of suberin or other lipid-like compounds, which can be misidentified as Klason lignin using the NREL method.[63,64] In order to prevent this overestimation, researchers have attempted to quantify these lignin through other methods. For barks, suberin can be depolymerized first through methanolysis, and then extracted with DCM, dried, and measured gravimetrically.[65] For seed coats, the ^{13}C NMR method can be used to approximate the C-lignin amount, *i.e.*,

the lignin content (weight%) in vanilla seed coats, which contains almost 100% C-lignin units, decreases from 65.4% (Klason lignin) to 13% when using the ^{13}C NMR method, as indicated in Table S1 and Table 1.[44] However, unlike Klason lignin, these methods are still not widely accepted for accurate quantification of lignin in barks and seed coats.

Barks contain a unique lignin unit of suberin, as well as H, G, and S lignin units.[53,66] Suberin is generally present in most barks and roots. However, some plant species also have suberin in other parts, such as fruit skins of pears, seed coats of *Arabidopsis thaliana*, and skins of root species like carrot or potato where suberin accounts for 20–50 weight% of dry biomass.[67–69] Suberin functions as a physiological protective barrier for plants due to its hydrophobic properties to retain water, insulate, and protect against pathogenic microbial attack.[68,70] In RCF, suberin can be converted further into aliphatic monomers, such as fatty acid methyl esters (FAMEs) and dimethyl esters.[65] Suberin content differs across wood
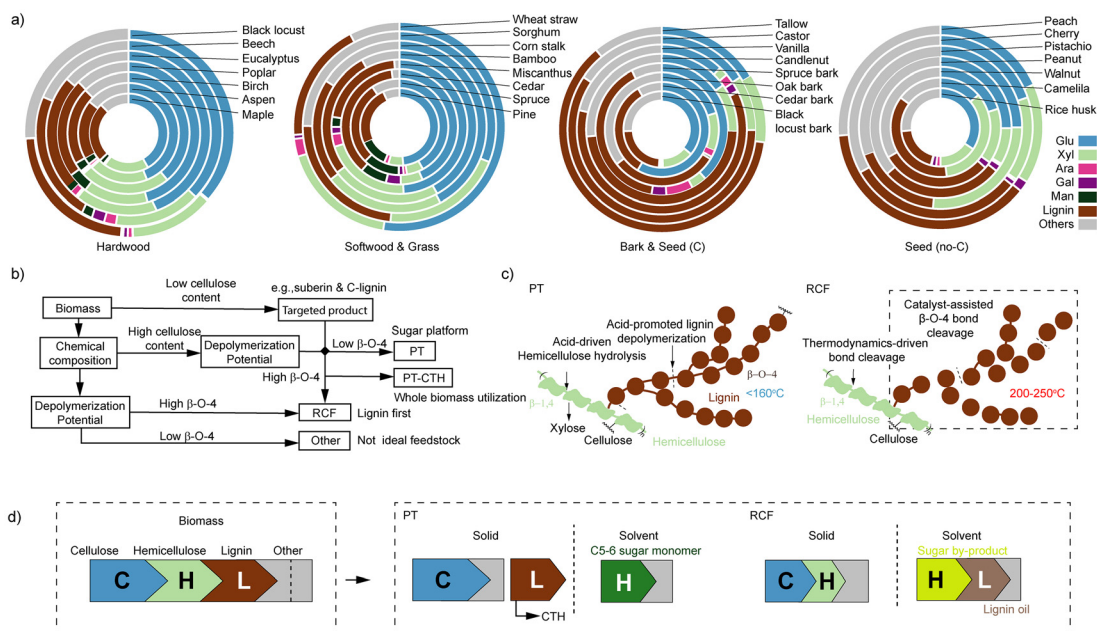
Fig. 3 (a) Plant part classification and chemical composition (weight%) of different biomass, including hardwood, softwood, grass, bark, and seed (with or without C-lignin). Data are taken from Table S1.[18–50] (b) Decision framework for biomass processing based on cellulose content and lignin depolymerization potential. (c) Mechanisms of lignin–hemicellulose dissociation during pretreatment (PT) and reductive catalytic fractionation (RCF). PT relies on acid hydrolysis under mild conditions, while RCF involves high-temperature catalytic β-O-4 cleavage. (d) Phase distribution of biomass components after PT and RCF. PT enables full separation of cellulose, hemicellulose sugars, and lignin; RCF yields lignin oil and sugar by-products in the solvent phase.

species. For example, suberin is high in some hardwood barks like cork oak bark (32.2–58.6%) and silver birch bark (37.0–60.0%), but it is low in poplar bark (3%) and willow bark (1.82%). Meanwhile, the ratio of H/G/S may depend on the type of wood of the plant species. For example, the bark of pine (softwood) contains low suberin (1.5–2.5%) and an H/G ratio of 0.25–0.59, while barks of eucalyptus and teak (hardwood) contain lignin with an S/G ratio of 0.8.[53]

Catechyl-lignin (C-lignin) was first discovered in seed coats of vanilla orchid and *Melocactus* genus in 2012. In seed coats of *Vanilla planifolia*, benzodioxane constitutes 98% of dimeric units from 2D NMR analysis, indicating that the lignin is almost exclusively composed of C-lignin and no S–G lignin units.[60] This phenomenon is most likely due to the absence of the *O*-methyltransferase (OMT) compound in the vanilla species, thereby preventing the pathway to convert C-lignin into G-lignin and subsequently S-lignin.[44,60] Following these studies, Li *et al.* (2018) attempted to extract the valuable catechyl monomer units through combinations of enzymatic pretreatment and RCF.[44] Out of 13% C-lignin w/w of vanilla seed coats, 88.6% monomer yields with 89% selectivity towards catechylpropanol was successfully achieved through RCF with a Pd/C catalyst and methanol solvent. This monomer yield is higher than the maximum monomer yields achieved through depolymerization of plant species with natural (S + G) lignin-units (±50%) and with genetically modified (high-S) poplar (78%).[26,44] Due to the high potential of C-lignin depolymerization, some studies attempted to depolymerize C-lignin of seed

coats in castor, Chinese tallow, jatropha, and candlenut in the Euphorbiaceae family, which were found to have high C-lignin units.[42,45,46,48,61,71,72]

3. PT-CTH and RCF of hardwood, softwood, grass, barks, and seed coats

In this section, we review the treatment conditions, delignification kinetics, monomer/oligomer yields, carbohydrate recovery, and monomer selectivity on PT-CTH and RCF processes over five biomass species.

3.1. Pretreatment followed by catalytic transfer hydrogenolysis (PT-CTH)

Pretreatment includes two major components, *i.e.*, physical and chemical processing. The physical treatment involves various approaches to break down biomass particles, such as ultrasound, microwave, extrusion, and milling, while chemical treatments are critical to cleave the linkages among the building block chemicals.[3] As the effectiveness of physical separation relies heavily on the chemical reactions in biorefineries, we emphasize the chemistry of biorefining in this review. The goal of pretreatment is to increase accessibility of the substrate to allow chemicals or enzymes for effective conversion.[73] This process reduces cellulose polymerization, destroys cellulose crystallinity, and increases the surface area and pore size of the substrates.[74] Pretreatment also separates cellulose from

lignin, preventing the inhibition caused by lignin during enzymatic hydrolysis of cellulose into residual sugars.[73]

Various chemical(s)[75,76] and solvent(s)[77,78] have been applied to catalyze the reaction and to dissolve the fractionated lignin and hemicellulose, respectively. The Kraft pulping process (Na$_2$S and NaOH in 145–170 °C) can be considered as the most representative pretreatment technique for delignification.[79] It has outstanding lignin removal efficiency (about 90%) and hence is widely applied in the pulping industry.[80] In the Kraft and other alkali pretreatment processes, lignin is removed from the cellulosic/hemicellulose bundles *via* significant ether bond breakage, lignin degradation and condensation.[81] Kraft and alkali-based pretreatment processes, including the ammonia fiber explosion (AFEX) process,[82] provide high quality polysaccharides to favor paper, polymer, and sugar production after further processing. However, as those processes can result in more severe and uncontrollable condensation issues on the fractionated lignin, they are considered less favorable in lignin-first application. Acid-catalyzed pretreatment processes include a few different variations, *e.g.*, organic solvents (organosolv),[83] deep eutectic solvents (DES),[84] and co-solvent enhanced lignocellulosic fractionation (CELF).[85] In these processes, easily hydrolysable acetyl groups are removed from hemicellulose branches linking between cellulose and lignin, providing opportunities to better preserve useful C–O–C structures in lignin for depolymerization. To narrow the focus of this review, we discuss mainly the acid-based organosolv and DES pretreatment processes.

3.1.1. Organosolv pretreatment. In organosolv pretreatment, numerous types of organic solvents have been used with acid catalysts for LCB fractionation. The most commonly applied organosolvs include glycerol, ethylene glycol, butanol, methanol, ethanol, and other alcohols. Organic acids (such as oxalic acid, formic acid, acetylsalicylic acid, acetic acid, and salicylic acid) and mineral acids, such as HCl, H$_2$SO$_4$, and H$_3$PO$_4$, are often employed as catalysts to speed up delignification and hemicellulose removal.[74] Other organosolv pretreatment approaches include the utilization of tetrahydrofuran (THF), γ-valerolactone (GVL), and 2-methyltetrahydrofuran (2-MeTHF), which show even better delignification performance.[83] Some organosolvs have the ability to prevent lignin condensation. For example, formaldehyde protects α-hydroxyl groups by forming 1,3-dioxane in Cα and Cγ, and diol forms ether linkages with Cα.[26,86] Organosolv pretreatment has been studied extensively as shown in Table S2.

3.1.2. Deep eutectic solvent (DES) pretreatment. DESs are generally produced through mixing two components, *i.e.* hydrogen bond donor (HBD) and hydrogen bond acceptor (HBA). Examples of HBDs include amines, carboxylic acids, alcohol, and carbohydrates, while examples of HBAs include quaternary salts like choline chloride (ChCl). HBAs and HBDs are solid forms at room temperature and become liquid when two reagents are combined. The eutectic temperature of various acidic DESs can be found in a review conducted by Qin *et al.*[87] DESs have similar properties to ionic liquids (ILs), but with greener attributes, *i.e.* non-toxic, biodegradable, and

biocompatible.[88–90] The recent studies on acid-based DES pretreatment of hardwood, grass, and seed coats are compiled in Table S3. Like organosolvs, DESs can be classified into three pH categories, *i.e.*, acid, alkali, and neutral. DESs have been found to be suitable solvents for pretreatment of LCB due to their high lignin dissolution ability.[89] Interestingly, DESs have also been utilized in RCF as a substitute for solvents. Comparison between organosolv and DES pretreatment in terms of reaction parameters and efficiency is shown and explained in further detail in the SI (Table S4).

3.1.3. PT-CTH efficiency in various biomass feedstocks. After pretreatment, hydrogenolysis (CTH) or solvolysis is used to stabilize the lignin and oligomer ether bonds by cleaving them into monomers.[91] Primarily, CTH is added to enable utilization of remaining lignin after pretreatment and thus, it aims to produce the highest monomer yield from lignin. Lignin fractionated from the biomass is suitable for depolymerization into phenolic monomers, if the pretreatment is efficient enough to extract lignin with the maximum amount of native linkages, particularly β-O-4 and/or benzodioxane.[77]

CTH efficiency is dependent on reaction conditions like temperature, pressure, catalyst, and solvent. Cellulose recovery, hemicellulose dissolution, delignification, and monomer yield of PT-CTH are listed in Table S2 for organosolv (from 32 studies)[26,42,45,48,72,77,83,86,92–119] and Table S3 for DESs (from 12 studies).[44,47,84,88,120–127] The monomer yield and carbohydrate recovery of PT-CTH of five LCBs are shown in Fig. 3e. Note that some of the monomer yields are not given in the literature and thus approximated from the β-O-4 content using the equation from Phongpreecha *et al.*,[101] and the carbohydrate recovery here includes the amount of carbohydrate remaining in the solid residue and the hemicellulose derivatives dissolved in the pretreatment liquor. Some calculations were performed to convert the units to g/g-biomass and to determine the carbohydrate recovery (Appendix 5 in the SI).

Since the main objective of PT-CTH is whole-biomass utilization, we evaluated cellulose yield, hemicellulose yield, and monomer yield to evaluate the total utilization in each biomass (Fig. 4). Across all biomass feedstocks, PT exhibits high efficiency in extracting cellulose and hemicellulose, but CTH efficiency is still low, only utilizing 3.2–10.4% of lignin. Seed coats with C-lignin have the highest average monomer yield of 7.0% g/g-biomass, compared to all other biomass types. This is because benzodioxane is preserved during acid pretreatment, while the β-O-4 content generally decreased. However, the PT-CTH data in this analysis only include acid pretreatment. Under base pretreatment, the benzodioxane structure may be partially cleaved.[72]

It is also observed that the range of monomer yields of seed coats is very broad, from 0.02 to 0.13 g/g-biomass. This is mainly because the monomer yield is highly dependent on C-lignin content, but C-lignin contents in seed coats (in g/g-biomass) have large margins *e.g.*, 4.6% in castor, 13% in vanilla, and 15.4% in Chinese tallow from the ^{13}C NMR results, as shown in Table 1. When the monomer yield is calculated based on g/g-C-lignin, the range of monomer yield is
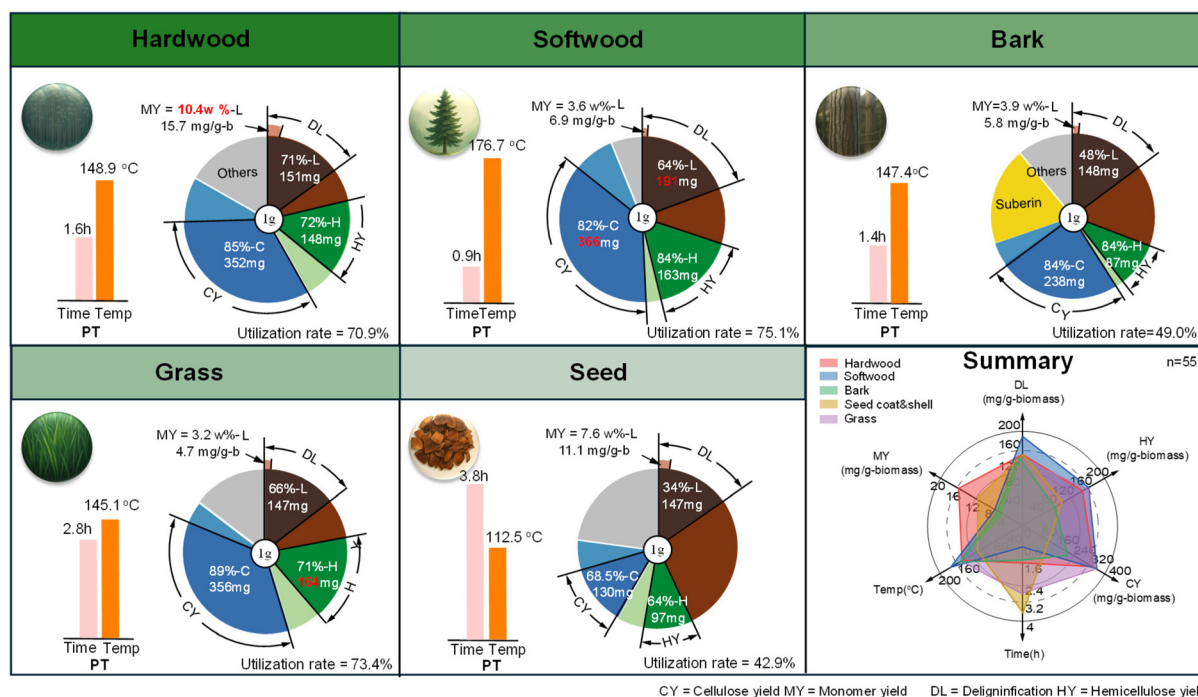
Fig. 4 Component fractionation performance of five representative biomass types (hardwood, softwood, bark, grass, and seed) under organosolv pretreatment. Pie charts illustrate the distribution and recovery of lignin (L), hemicellulose-derived sugars (H), cellulose (C), and lignin-derived monomer yield (MY) per g of raw biomass. Bar charts show the corresponding organosolv pretreatment conditions. DES-based pretreatment showed comparable performance to organosolv methods, with detailed comparisons available in Table S4 (not shown here). The radar chart summarizes the biomass utilization potential and separation difficulty across different feedstocks. A total of n = 55 data points are included in this figure. Other experimental conditions and pretreatment performance, including solid loading, acid type, and acid dosage, are listed in Table S2.

Table 2 RCF setups and results summarized with illustration of the effects of solvents

Feedstock	Catalyst	Solvent	H source	Monomer yield	Ref.
Poplar	RANEY® Ni	Ethyl acetate	From solvents	26%	133
		Acetone		17%	
		Methanol		12%	
Cotton stalks	Ru/HY zeolite	Ethanol	H_2 (1–40 bar)	18% for 30 bar H_2	134
Pine sawdust	CuO/C	Dioxane	H_2 (3 MPa)	2%	135
		isopropanol		5%	
		Methanol		15%	
		Ethanol		7.7%	
Silver birch wood chips	0.15% Co/N–C	Ethanol	H_2 (3 MPa)	38.9%	136
		Methanol		48.3%	
		Isopropanol		28.9%	
		1-Propanol		35.4%	
		Tetrahydrofuran		19.1%	
Corn stover	Ni or Ru/activated carbon	Methanol	For 30 bar H_2	37.9% for Ru/C with H_3PO_4 added	137
Birch	Ru/C	Deep eutectic solvent of ChCl/EG	From solvents	59% for 10% EG–ChCl	138
Poplar	Ni/C	Methanol	6 MPa H_2	18% maximum	139
Poplar	5% Ru/C	Isopropanol (IPA)	From solvents	4.9%	140
		Methanol (MeOH)		17.9%	
		IPA : MeOH 1 : 1		17.3%	
		IPA : MeOH 7 : 3		12.2%	
		IPA : MeOH 3 : 7		16.6%	
Birch sawdust	Ni/Al$_2$O$_3$	Methanol	3 MPa H_2	44% maximum	141
Poplar sawdust	5% Ru/C (RCF)	Methanol	3 MPa H_2	25%	9
	5% Ru/C (ARCF)	Ethylene glycol	From solvent	25.8%	
Birch sawdust	5% Ru/C	Methanol	3 MPa H_2	52%	142
		Water	3 MPa H_2	25%	

0.71–0.84.[42,44,45,47,48,62,72] Across all biomass feedstocks except seed coats, low monomer yields are observed after PT-CTH, but utilization of protection agents like formaldehyde during PT (OS-P) can significantly increase the monomer yield. For PT-CTH of barks, only the phenolic monomer yield from lignin is included.

3.2. Reductive catalytic fractionation (RCF)

RCF is a lignin-first approach for the conversion of biomass into value-added aromatics. Lignin's physical location and activity in biomass composites make it possible to extract and depolymerize it into phenolic monomers, dimers, and oligomers. The performance of β-O-4 unit cleavage and its stabilization are catalyst-specific.[128] RCF consists of three significant stages: solvo-thermal fractionation of lignin from biomass, depolymerization of the fractionated lignin into phenolic monomers, and monomer stabilization.[129] Studies have proposed that the fractionation primarily occurred through solvolysis (*e.g.* methanol in 200–250 °C), while the depolymerization and monomer stabilization occurred through hydrogenation by catalysts (*e.g.*, Ru/C) and H_2 gas.[43,130] Without the presence of reductive catalysts, β-O-4 cleavage leads to repolymerization and stable C–C bonds. After repolymerization, the condensed lignin is intended to be inert and incapable of being cleaved under RCF conditions.[131] This section will first discuss the effects of solvents in RCF, and then evaluate the RCF performance on hardwood, softwood, grass, barks, and seed coats.

3.2.1. Effects of solvents on monomer yield. The catalysts and solvents used in the recent RCF studies are listed in Table 2. Generally, polar solvents with strong protonating capability (*e.g.* carboxylic acids) favor both the fractionation of lignocellulose and the fragmentation of lignin due to active intermediates formed after the protonation of hydroxyl groups in lignin, but inhibiting repolymerization between these reactive protonated species can be relatively difficult, especially in acidic environments at elevated temperatures compared to neutral conditions.[132]

In contrast, alcohol solvents that are less protic typically assist the RCF process by acting as *in situ* hydrogen donors while exhibiting promising solubility for lignin.[143] Most alcohol solvents are also capable of stabilizing lignin monomers formed *via* the formation of acetals or other protecting groups with reactive phenolic aldehydes, which is especially prominent when diols are used.[144] Since the Cα–OH group in lignin is prone to be eliminated and form carbocations that easily bind with other units during the depolymerization phase of RCF, Zhang *et al.* utilized the etherification between Cα–OH and ethylene glycol (EG) and acetalization of aldehyde monomer products to suppress side reactions. Their kinetic analysis for reaction pathways implies that when the temperature increases, EG still acts as an excellent stabilizing agent for the acidolysis of lignin.[144] Therefore, the mixed usage of both acids and alcohols can have synergistic effects for improving RCF performance.

Wang *et al.* discovered that when using methanol as a solvent for poplar lignin RCF, its etherification with Cα and Cγ

hydroxyl groups to form a methoxy group is prominent for lignocellulosic feedstock, yet the presence of a CuO/C catalyst can effectively inhibit the further methoxylation of obtained monomers with OH groups.[135] Li *et al.* conducted the control experiments for a Co/N–C catalyst with a bare support or N-free catalyst tested for RCF, and it turned out that the monomer yields of using N–C and Co/C dropped from nearly 50% to 8.1% and 19.9% respectively. They also found that N-doping might facilitate the breakage of C–O bonds and C=C double bonds in lignin.[136] Anderson *et al.* investigated the co-catalysis of homogeneous weak acids for RCF of corn stover in 2016. When H_3PO_4 was added, the monomer yield increased from 28.6% to 37.9%, among which methyl coumarate was the compound with the highest increment in quantity.[137] Overall, the direct supply of hydrogen and utilization of traditional hydrogenation catalysts such as Ru or Ni based complexes were widely adopted in previous studies on RCF. Yet, several trials under hydrogen-free conditions with these catalysts also achieved decent RCF performance in terms of monomer yields. For instance, Li *et al.* confirmed the feasibility of achieving efficient hydrogen transfer from solvents during lignin hydrogenolysis *via* the tuning of HBA. The EG and HBA used in this study formed a DES system during RCF where the hydrogen donating rate can be adjusted simply by changing the EG : HBA ratio.[138]

3.2.2. RCF efficiency in various biomass feedstocks. A total of 26 RCF studies were analyzed in terms of monomer yield, monomer selectivity, oligomer yield, carbohydrate retention, and by-products. References and reaction parameters of the RCF are compiled in Table S5.[14–17,25,28,36,40,41,43,44,62,65,71,128,141,142,145–163] Except for seed coats, average reaction parameters are similar across all biomass feedstocks, *i.e.*, 212–234 °C temperature, 3.1–4.0 h reaction time, 10.8–12.1% catalyst dosage, 32–36 bar, 4.3–5.8% solid loading (Table S6). The biggest differences in the RCF of seed coats are 23.8% catalyst dosage and 0.8% solid loading, which indicate that the process requires much higher amounts of catalyst and solvent. The temperature used in all RCF reactions ranges from 180 to 250 °C, possibly because hemicellulose starts decomposing to oligomeric C_5 derivatives at 180 °C.[164]

As lignin is the priority in most RCF studies, we analyzed RCF efficiency based on monomer yield and monomer selectivity. We also investigated the carbohydrate recovery in the RCF pulp to evaluate its sustainability. Here, carbohydrate recovery is the carbohydrate retention, which is the cellulose and hemicellulose remaining in the RCF pulp. Each parameter is presented in absolute value (*i.e.*, g/g-dry-biomass) and relative value (*i.e.*, g/g-lignin, g/g-carbohydrate, and g/g-monomer) to allow comparison between five different types of biomass feedstocks. The collected data are shown in Tables S7 and S8. Average values are listed in Table 3 and illustrated in Fig. 5. Some calculations were performed, mainly for unit conversion, such as from g/g-lignin to g/g-biomass, and for quantification of by-products.

In terms of monomer yield (g/g-lignin), the RCF of seed coats produces the highest yield, with an average of 64.1 ±

Table 3 Average and standard deviation of RCF data. All values are in weight%. Average values of RCF data in Fig. 3e. All values are listed in Table S5

No	Biomass	Cell	Hem	Lig	Sub	Oth	Mono (g/g-bio)	Mono (g/g-lig)	Olig (g/g-bio)	Olig (g/g-lig)	Pulp (g/g-bio)	Carb ret (g/g-carb)	Carb ret (g/g-bio)	By-prod (g/g-bio)
1	Hardwood	42.5 ± 3.4	19.45 ± 2.5	21.6 ± 3.2		15.3 ± 4.5	9.3 ± 1.7	44.0 ± 9.4	8.3 ± 1.5	39.3 ± 13.4	58.2 ± 3.2	76.9 ± 13.4	47.6 ± 7.9	23.4 ± 10.5
2	Softwood	45.7 ± 3.6	16.6 ± 5.3	28.6 ± 3.4		9.0 ± 2.9	4.4 ± 1.1	15.9 ± 5.0	7.6 ± 1.4	31.0 ± 10.2	75.2	67.8 ± 10.2	46.5 ± 7.0	32.8 ± 5.6
3	Grass	37.97 ± 5	23.4 ± 2.3	17.6 ± 3.2		21.0 ± 8.8	4.5 ± 1.6	25.4 ± 6.3	3.6 ± 0.8	23.2 ± 16.9	59.4	63.0 ± 16.9	40 ± 12.9	29.8 ± 6.7
4	Barks	24.17 ± 8	11.4 ± 1.5	26.8 ± 4.3	19.3 ± 11.8	21.6 ± 6.2	2.2 ± 1.3	7.9 ± 4.7	6.0 ± 0	24.0	43.0	62.5	22.2 ± 5.7	43.7
5	Seed coats	13.87 ± 1.6	7.97 ± 2.7	58.5 ± 4.5		20.3 ± 4.2	6.1 ± 2.5	64.1 ± 18.2	5.4 ± 5.4	34.5	65.8	63.6	12.0 ± 1.8	55.8 ± 2.5
	Barks (suberin)			19.3 ± 11.8			5.3 ± 2.4	40.9 ± 25.2						
	Seed coats (NC)	22.3 ± 6.2	20.2 ± 7.3	28.8 ± 7.2		28.7 ± 6.6	6.9 ± 2.5	25.1 ± 9.5						

Abbreviations: g/g-bio = g/g-dry-biomass; g/g-lig = g/g-Klason-lignin-in-dry-biomass; Lig = lignin in the dry biomass; Sub = suberin in the dry biomass; Oth = others (other components) in the dry biomass; Mon = monomer yield of RCF; Olig = oligomer yield of RCF; Carb ret = carbohydrate retention after RCF; By-prod = by-product of RCF process. NC = no C-type lignin; Cell = cellulose in the dry biomass; Hemi = hemicellulose in the dry biomass; Pulp = pulp yield of RCF; Mono = monomer yield of RCF; Olig = oligomer yield of RCF; the parameters are calculated through the equations shown below. Note that the calculation is only used for calculating others (g/g-biomass), by-product (g/g-biomass), conversion of units from g/g-lignin to g/g-biomass or *vice versa*, and conversion of units from g/g-carbohydrate to g/g-biomass or *vice versa*. All other values are compiled directly from literature.

$$\text{Others}\left(\frac{\text{g}}{\text{g}_{\text{biomass}}}\right) = 1 - \text{Cellulose} - \text{Hemicellulose} - \text{Lignin} - \text{Suberin}$$

$$\text{Monomer yield}\left(\frac{\text{g}}{\text{g}_{\text{biomass}}}\right) = \text{Monomer yield}\left(\frac{\text{g}}{\text{g}_{\text{lignin}}}\right) \times \text{Klason lignin in biomass}\left(\frac{\text{g}_{\text{lignin}}}{\text{g}_{\text{biomass}}}\right)$$

$$\text{Oligomer yield}\left(\frac{\text{g}}{\text{g}_{\text{biomass}}}\right) = \text{Oligomer yield}\left(\frac{\text{g}}{\text{g}_{\text{lignin}}}\right) \times \text{Klason lignin in biomass}\left(\frac{\text{g}_{\text{lignin}}}{\text{g}_{\text{biomass}}}\right)$$

$$\text{Carbohydrate retention}\left(\frac{\text{g}}{\text{g}_{\text{biomass}}}\right) = \left(\frac{\text{Mass}_{\text{carbohydrate remained in pulp}}}{\text{Mass}_{\text{dry biomass}}}\right)$$

$$\text{Carbohydrate retention}\left(\frac{\text{g}}{\text{g}_{\text{carbohydrate}}}\right) = \left(\frac{\text{Mass}_{\text{carbohydrate remained in pulp}}}{\text{Mass}_{\text{cellulose and hemicellulose in dry biomass}}}\right)$$

$$\text{Byproduct}\left(\frac{\text{g}}{\text{g}_{\text{biomass}}}\right) = 1 - \text{Monomer} - \text{Oligomer} - \text{Carbohydrate retention} - \text{Others}$$
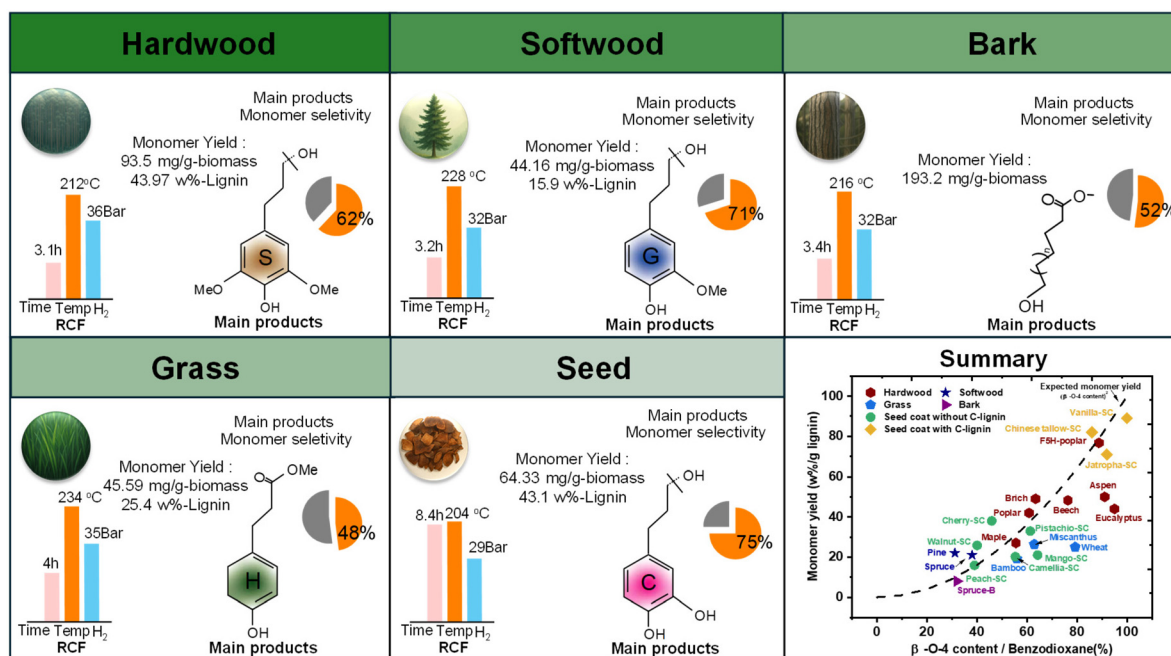
Fig. 5 RCF performance of five representative biomass types (hardwood, softwood, bark, grass, and seed). Bar charts show the average reaction conditions, including temperature, time, and hydrogen pressure taken from Table 3. Chemical structures illustrate the dominant lignin-derived monomer types taken from Table S8. Hardwood primarily yields S-type monomers, softwood produces G-type monomers, bark generates long-chain unsaturated hydrocarbons derived from suberin, grass yields H-type fatty acid (FA) monomers, and seed biomass can produce C-type lignin monomers. The scatter plot highlights the correlation between β-O-4 or benzodioxane linkage abundance and monomer yield (data from Table S1), indicating that lignin structural features can serve as predictors of depolymerization efficiency. The black dotted line is the expected monomer yield based on the equation proposed by Phongpreecha *et al.*[101] *i.e.*, (β-O-4 content)^2.

18.2% g/g-C-lignin (equivalent to 6.1 ± 2.5% g/g-biomass), followed by hardwood, suberin-in-barks, grass, seed coats (without C-lignin), softwood, and lignin-in-barks. However, it should be emphasized that this value (seed coats) is based on g/g-C-lignin measured by ^{13}C NMR, while the values of other biomass feedstocks are based on g/g-Klason-lignin in biomass. Although not an accepted method yet, the ^{13}C NMR method is currently used to predict C-lignin content in most recent studies on seed coats.[44,47,62] To allow for comparison between the five LCBs, the monomer and oligomer yields of seed coats were calculated in g/g-C-lignin and g/g-biomass. When the monomer yield is calculated based on g/g-biomass, hardwood produces the highest monomer yield of 9.3 ± 1.7%.

The Klason lignin and suberin in barks are separated in our analysis. This results in a comparable g/g-Klason-lignin value with the other LCBs *i.e.*, hardwood, softwood, and grass. RCF of suberin resulted in 40.9 ± 25.2% aliphatic monomer, but RCF of lignin in barks produced only 7.9 ± 4.7% g/g-lignin phenolic monomer. This suggests that barks have higher potential for aliphatic monomer production *e.g.*, fatty acid methyl esters (FAME), OH–FAMEs, dimethyl ester, or other lipid derivatives.

Limited data are available for oligomer yield and carbohydrate retention of barks and seed coats; therefore, some assumptions were made to approximate these values *e.g.*, 62.5% g/g-carbohydrate was approximated for barks,[65] while 63.6% g/g-carbohydrate was assumed for seed coats[165] (details

of these assumptions are listed in Table S5). In both aspects, hardwood has the highest oligomer yield and the highest carbohydrate retention, followed by softwood and grass. Significantly lower values of RCF carbohydrate retention were observed for barks (22.2%) and seed coats (12.0%), due to their inherently low carbohydrate content. Barks have a high lignin content left behind as a by-product in the RCF solid residue (pulp), *i.e.*, out of 36% lignin (g/g-biomass) in black locust bark, 21% lignin (g/g-biomass) remained in the bark residue after RCF.[65] For seed coats, the high lipid content was mostly extracted during the pre-extraction (*e.g.*, with water/acetone) or converted into lipid derivatives after RCF, which is usually unquantified and unaccounted for as a product.[71,154,155]

4. Discussion

4.1. Biomass potential based on β-O-4/benzodioxane and cellulose content

Due to the unique chemical composition of each biomass, the biomass potential for monomer production was evaluated for each species. The proportion of β-O-4/benzodioxane linkages in lignin was investigated (Table S1) and theoretical RCF monomer yield was predicted based on the model proposed by Phongpreecha *et al.* (black dotted line, Fig. 5).[101] It can be observed that the correlation between β-O-4/benzodioxane

content and monomer yield of the RCF data collected in this study is consistent with the model proposed by Phongpreecha *et al.*[101] We then constructed a scatter plot (Fig. 6) to illustrate the potential of each biomass for monomer production, solely based on theoretical monomer yield and cellulose content. The scatter plot is then divided into four quadrants, each of which suggests a recommended process for different biomass species, *i.e.*, PT, PT-CTH, RCF, or others.

From the discrepancy of RCF monomer yield between hardwood and softwood, a high S/G ratio also seems to increase the monomer yield. However, Anderson *et al.* (2019) conducted flow-through RCF in five natural poplar variants with S/G ratios ranging from 1.41 to 3.60 and found that there is no correlation between the S/G ratio and the monomer yield at 50% lignin extraction.[166] All poplar samples with different S/G ratios were depolymerized to 32% monomer yields, at 80% lignin extraction. To explain these findings, the study hypothesized that the initial monomer concentrations across all biomass variants were of similar value, prior to bio-lignification. In the lignification process, the slow addition of monomer reduces the dimerization (C–C bond linkage) and increases the amount of β-O-4, which subsequently increases the monomer yield. The study concluded that the monomer yield is affected by the C–O or C–C bond formation during the lignification process.[166] Furthermore, Guo *et al.* (2017) suggested that the higher amount of β-5 and the higher molecular weight of softwood may be the main reasons behind the low depolymerization yield.[164] From

these observations, it can be inferred that instead of the S/G ratio, the monomer yield is more affected by the amount of C–O bonds (*e.g.*, high β-O-4/benzodioxane) and C–C bonds (*e.g.*, low β-5) in the biomass. These findings are consistent with the theoretical monomer yield model used by Phongpreecha *et al.*[101]

4.2. Monomer yield and carbon utilization

The ranges of monomer yield and carbohydrate recovery rate for RCF and PT-CTH are shown in Fig. S1. Mass balance analysis was conducted based on average values of the data for monomer yield, oligomer yield, carbohydrate retention, and by-product (all values are in %g/g-biomass). The results of the mass balance are illustrated in Fig. 7. Sankey diagrams were drawn to illustrate the fate of each component in hardwood after PT-CTH and RCF (Fig. 7a and b). The mass balance analysis for RCF (Fig. 7c) showed that hardwood has the highest yield across all parameters *i.e.*, 9.3% monomer yield, 8.3% oligomer yield, and 47.6% carbohydrate recovery (in the unit of %g/g-biomass). The mass balance of PT-CTH does not include the PT-CTH with protection of β-O-4 (*e.g.*, formaldehyde,[26] propionaldehyde,[167] and *p*-toluene sulfonic acid[23]) where the monomer yield will be close to the RCF value, as shown in Fig. S1.

Across most biomass types, RCF produces higher monomer yield, except for seed coats with benzodioxane, and PT-CTH exhibits higher carbon utilization (Fig. 7d). Separation of the dissolved lignin and hemicellulose derivatives (such as xylose) in PT-CTH can simply be performed *via* lignin precipitation or extraction prior to the hydrogenolysis process. This is followed by the efficient hydrolysis of cellulose in the solid residue of PT-CTH into glucose. Due to these reasons, the C_{5-6} sugar derivatives from cellulose and hemicellulose are considered as utilizable in PT-CTH, resulting in higher total utilizable products in PT-CTH. On the other hand, C_{5-6} sugar derivatives are treated as a by-product (usable with limitations in Fig. 7d) in RCF, as it is required to separate the derivatives from the lignin oil first before it can be utilized. RCF pulps contain high fractions of carbohydrate and are present in high quantities after the reaction (43.0–75.2% of initial biomass weight). However, in the lignin-first biorefinery process, RCF pulps are generally not hydrolyzed to C_{5-6} sugar in most studies. Therefore, they are considered as usable with limitations. Nevertheless, it is important to note that although most RCF studies do not evaluate the potential utilization of C_{5-6} sugar derivatives, some studies have successfully extracted and utilized these derivatives from RCF.[25,36,142,145,150,151]

4.3. Monomer selectivity

Monomer selectivity for different combinations of solvents and catalysts was analyzed for all five types of LCBs. The average value of the highest selectivity towards specific monomers in RCF was calculated for each LCB (Fig. 5). The average was calculated from the selectivity of major monomers produced in 21 different studies, as listed in Table S8.[15–17,25,26,28,36,41,43,44,65,71,141,142,152,154,155] As expected,
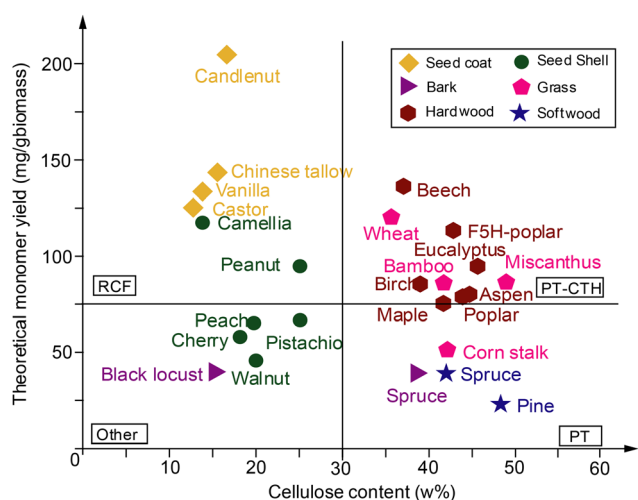

Fig. 6 A two-dimensional compositional map showing the relationship between lignin depolymerization potential (*x*-axis) and cellulose content (*y*-axis) across diverse biomass feedstocks. Samples are grouped into four quadrants, each suggesting a preferred valorization route: PT-CTH for carbohydrate- and β-O-4-rich species (Quadrant I, *e.g.*, poplar and miscanthus); direct RCF for lignin-rich, low-carbohydrate feedstocks (Quadrant II, *e.g.*, candlenut and castor); thermochemical or extractive routes for low-reactivity, low-carbohydrate biomass (Quadrant III, *e.g.*, walnut shell and black locust); and cellulose-focused pretreatment for softwood with recalcitrant lignin (Quadrant IV, *e.g.*, pine and spruce). Data can be referred from Table S1.
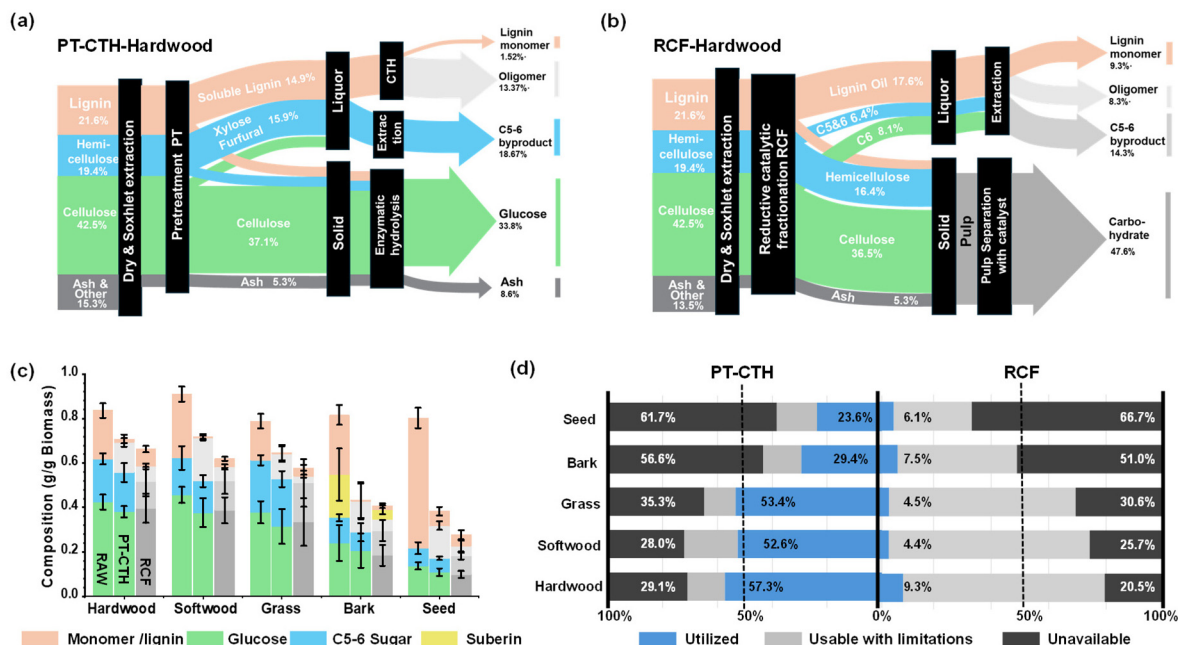
Fig. 7 Sankey diagram depicting the mass balance of (a) PT-CTH of hardwood and (b) RCF of hardwood. (c) Average values of the initial composition of biomass (Raw), product composition after PT-CTH, and product composition after RCF. For the initial composition of biomass (Raw), the four components are lignin (converted to a monomer), hemicellulose (converted to a C_5 sugar), cellulose (converted to glucose and a C_6 sugar), and suberin (converted to an aliphatic monomer). (d) Average values of utilizable products (utilized), possibly usable products (usable with limitations), and lost by-products (unavailable) after PT-CTH and RCF. Note that the mass balance does not include the PT-CTH with protection agents (*i.e.*, OS-P) to better represent the general PT-CTH in the literature. The mass balance is calculated based on Table 3 for RCF and the average values obtained from Tables S2 and S3 for PT-CTH. Calculation methods for the mass balance are shown in Appendix 5 in the SI.

the choice of feedstock affects the monomer selectivity for both RCF and PT-CTH *i.e.*, hardwood produces propyl-/propanol-G/S (62%), softwood produces propyl-/propanol-G (69%), grass produces methyl-dihydro-F/pC (43%), lignin in barks produces propyl-/propanol-G/S (31%), suberin in barks produces OH-FAMEs (49%), and seed coats produce propyl-/propanol-C (76%). On the other hand, the monomers produced after PT-CTH are vastly distinct across different pretreatments, as shown in Table 4.

Selection of the catalyst and the solvent can considerably affect the RCF selectivity towards propyl-/propanol-monomers. Several studies have shown that Ru–C and Ni–C generally produced propyl-based monomers, while Pd–C catalysts typically produced propanol-based monomers. Our analysis showed similar results where we observed low standard deviations of monomer selectivity of RCF with methanol, Ru/C and methanol, Pd/C in hardwood (75 ± 6% propyl-G/S in Ru/C; 85% propanol-G/S in Pd/C), softwood (82 ± 1% propyl-G in Ru/C; 87 ± 3% propanol-G in Pd/C), grass (39 ± 6% propyl-F/pC in Ru/C), and seed coats (80 ± 9% propanol-C in Pd/C). We also observed that changes in solvents, setup, and catalyst-support can alter the selectivity towards other monomers. Changing the solvent from methanol to methanol/water in RCF with Ru/C changes the selectivity from 82% propyl-G to 55% propanol-G in pine, and increases selectivity towards ferulic acid and coumaric acid in grass.[16] RCF of eucalyptus in butanol/water with Ru/C produced 85% propanol-G/S, and

RCF of castor seed coats in ChCl/EG with Pd/C produced 89% propyl-C. When flow-through RCF (FT-RCF) with methanol is utilized, Ru/C alters the selectivity towards 65% propanol-G/S in poplar and 60% propanol-G/S in pine.[16] Finally, changing the catalyst support to Ni/Al$_2$O$_3$ produces 66% propanol-G/S in birch,[141] while Ru/CNT produces almost equal selectivity of propyl-based and propanol-based monomers in both hardwood and softwood.[17]

In contrast with other biomass types, PT-CTH of seed coats shows comparable selectivity of 71%–97%, when compared to RCF, due to the intrinsic acid-resistant benzodioxane in C-lignin. In biomass with S/G/H-type lignin, the reaction with an acid during pretreatment may have resulted in various monomers which are not obtained in RCF. Distinct products were generated in PT-CTH such as ethyl-S/G and methyl-ether-propyl-S/G/pC.[12,26,88,124] In the PT-CTH with a formaldehyde protection agent, 3-methyl-4-propyl-G/S was produced.[8] This implies that although the use of a protection agent to preserve β-O-4 during pretreatment increases the monomer yield, it may produce varying monomers and decrease monomer selectivity. On the other hand, it may be possible to produce the desired monomers by fine-tuning the pretreatment conditions. Finally, although the monomer selectivity of PT-CTH is lower than that of RCF, there are less C_5 and C_6 sugar by-products in PT-CTH. This leads to higher overall selectivity of monomers in the lignin oil from PT-CTH.

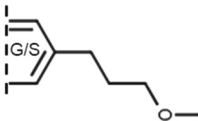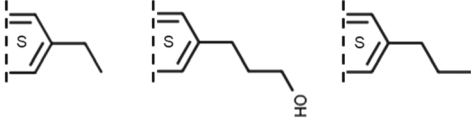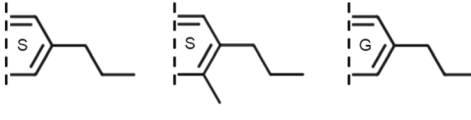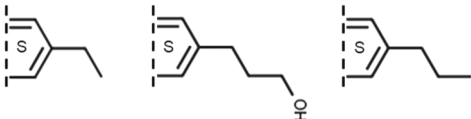**Table 4** Monomer selectivities of various PT-CTH studies
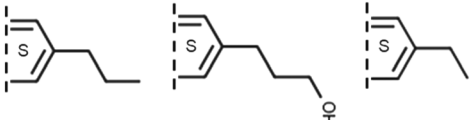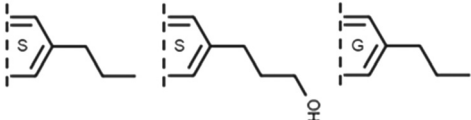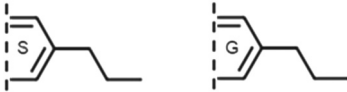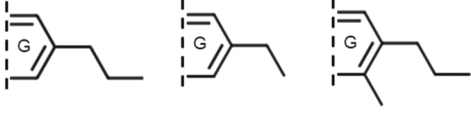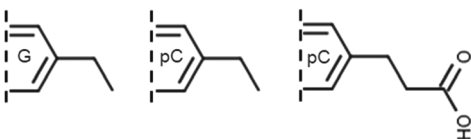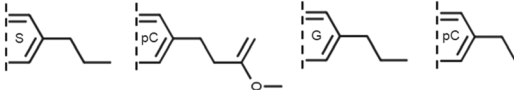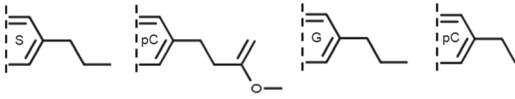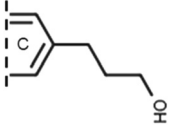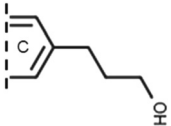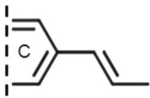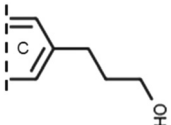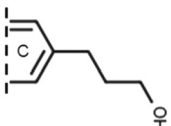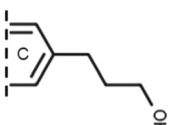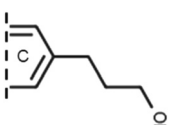
No	CTH substrate[a]	Solvent	Catalyst	Monomer[b]	Selectivity[c]	Ref.
1	Oak PT-OS Methanol/H_3PO_4 160 °C, 2 h	Methanol	Pd/C		78%	12
2	Beech PT-OS dioxane/HCl 80 °C, 5 h	THF	Ru/C		1: 29% 2: 28% 3: 26%	26
3	Beech PT-OS-P dioxane/HCl/*FA* 80 °C, 5 h	THF	Ru/C		1: 30% 2: 21% 3: 16%	26
4	Hi–S poplar PT-OS dioxane/HCl 80 °C, 5 h	THF	Ru/C		1: 61% 2: 11% 3: 23%	26
5	Hi–S poplar PT-OS-P dioxane/HCl/*FA* 80 °C, 5 h	THF	Ru/C		1: 24% 2: 21% 3: 20%	26
6	Birch PT-DES ChCl/OA (1 : 1) 120 °C, 0.5 h	Methanol	Ru/C		1: 91% 2: 9%	26
7	Birch PT-DES-P ChCl/*EG*/OA (1 : 2 : 0.2) 100 °C, 24 h	Methanol	Ru/C		1: 49% 2: 28% 3: 8%	26
8	Birch PT-DES-P ChCl/*EG*/OA (1 : 2 : 1) 80 °C, 0.5 h	Methanol	Ru/C		1: 73% 2: 9%	26
9	Spruce	Methanol	Ru/C		1: 60% 2: 10%	26
10	Spruce PT-OS-P dioxane/HCl/*FA* 100 °C, 2 h	THF	Ru/C		1: 37% 2: 33% 3: 9%	26
11	Sorghum PT-DES ChCl/LA (1 : 2) 145 °C, 6 h	Isopropyl alcohol	Ru/C		1: 16% 2: 15% 3: 13%	88
12	Bagasse PT-DES-P *L-Cys*/LA (1 : 10) 80 °C, 6 h	Methanol	Pd/C		1: 34% 2: 18% 3: 16% 4: 15%	124

Table 4 *(Contd.)*

No	CTH substrate[a]	Solvent	Catalyst	Monomer[b]	Selectivity[c]	Ref.
13	Bagasse PT-DES-P *L-Cys*/LA (1 : 10) 100 °C, 6 h	Methanol	Pd/C		**1**: 32% **2**: 20% **3**: 17% **4**: 18%	124
14	Castor sc PT-OS Ethanol/H_2SO_4 190 °C, 4 h	Methanol	Pd/C		82%	72
15	Castor sc PT-DES ChCl/LA (1 : 2) 100 °C, 6 h	Methanol	Pd/C		86%	72
16	Castor sc PT-OS Dioxane/HCl 85 °C, 3 h	Methanol	Ru/ZnO/C		72%	45
17	*C. tallow* sc PT-DES ChCl/EG/$AlCl_3$ 140 °C, 4 h	Methanol	Pd/C		95%	47
18	Jatropha sc PT-OS Dioxane/HCl 85 °C, 3 h	Methanol	Pd/C		97%	48
19	Vanilla sc PT-DES LiBr/HCl 160 °C, 2 h	Methanol	Pd/C		71%	44
20	Candlenut sc PT-OS 2-MeTHF/H_2O/HCl 160 °C, 2 h	Methanol	Pd/C		91%	42

[a] PT-OS = organosolv pretreated; PT-OS-P = organosolv pretreated with protection agent; PT-DES = deep eutectic solvent pretreated; PT-DES-P = deep eutectic solvent pretreated with protection agent; sc = seed coats with C-lignin; FA = formaldehyde; ChCl = choline chloride; EG = ethylene glycol; OA = oxalic acid; L-Cys = L-cysteine; LA = lactic acid. Protection agents like FA, EG, and L-Cys are bolded and italicized. [b] G = guaiacyl; S = syringyl; G/S = guaiacyl/syringyl; *p*C = *p*-coumaryl; C = catechyl. [c] The monomers are labelled chronologically from left to right *i.e.*, the leftmost is **1**.

4.4. Delignification kinetics

In PT-CTH and RCF, temperature plays a major role in influencing the reaction kinetics. For instance, Dong's study on diol pretreatment in eucalyptus at 160 °C achieved 93% lignin removal,[168] while Wang's study using *p*-toluene sulfonic acid with poplar at 80 °C achieved only 54.8% delignification within one hour.[97] This discrepancy underscores the substantial impact of temperature on lignin removal efficiency. To better illustrate the comparison, pretreatment conditions were categorized into high-temperature (HT, Temp > 170 °C), medium-temperature (MT, 100 °C < Temp < 170 °C), and low-temperature (LT, Temp < 100 °C) groups (Fig. 8). RCF reactions are also compared here. RCF reactions are relatively standardized, typically conducted at 200–250 °C (HT) under 20–40 bar H_2, yielding consistent kinetic profiles.

OS-PT-MT and DES-PT-MT pretreatment achieves the fastest lignin removal rates, consistently reaching over 80% removal within 60 minutes, as observed across multiple studies.[77,94,99] As the temperature decreases, the lignin removal efficiency
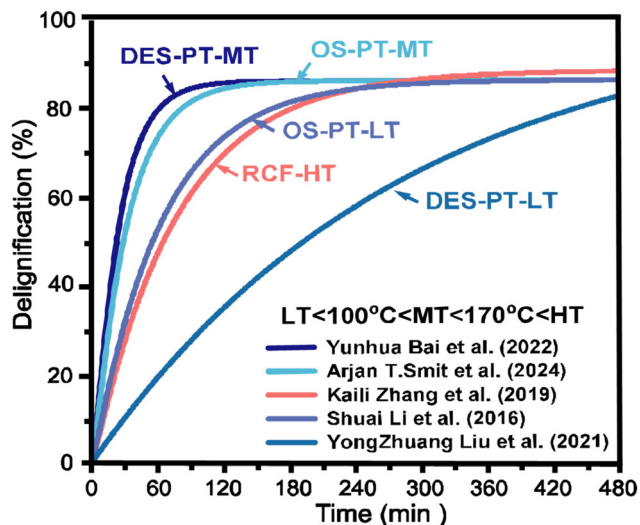
Fig. 8 Delignification kinetics in various pretreatment methods and RCF (Appendix 6 in the SI).[26,120,121,169,171]

gradually declines. Nonetheless, the presence of an acid in organosolv pretreatment enhances polysaccharide hydrolysis, allowing medium-temperature organosolv treatments to out-perform RCF in lignin removal speed. When RCF operates at elevated pressures and temperatures, it typically requires around 3 hours to reach 80% lignin removal.[169] Notably, DES-PT-LT treatments exhibit slower lignin removal kinetics; for instance, the study by Yu *et al.* (2018) reported only 37% removal after 6 hours.[170] In summary, medium-temperature pretreatment demonstrates the most rapid lignin removal kinetics, while low-temperature DES pretreatments offer potential for more controlled and gradual delignification.

4.5. Environmental and economic factors

To quantify environmental factors, we calculated the carbon economy and *E*-factor for RCF and PT-CTH across the five biomass species. For economic factors, cost–benefit analysis was performed. Parameters, assumptions, and calculation methods are shown in Appendix 7 in the SI.

4.5.1. Carbon economy. Here, carbon economy is the carbon utilization in biomass subtracted by energy consumption (both in $kg-CO_2e$). Some important assumptions are made for this calculation. Since the main objective is to compare RCF and PT-CTH in terms of energy, the boundary conditions are set only within the reaction itself and the subsequent solvent recovery, which are the main contributor to energy consumption. Other processes like pre-extraction of biomass and other downstream processes are not considered since they are assumed to be similar between RCF and PT-CTH. Carbon in all biomass feedstocks is assumed to be 45% from the CHNS-O analysis.[172] Fig. 9 shows the carbon economy comparison between PT, PT-CTH, and RCF.

Solvent recovery contributes to 70–80% of energy consumption in all cases, highlighting the importance to increase the solid loading in both RCF and PT-CTH to reduce the solvent per kg of biomass. In terms of biomass, softwood achieves the highest carbon economy in all processes, followed by hard-wood, grass, barks, and seed coats. For seed coats, high catalyst dosage (25.71% g/g-biomass) and low solid loading (0.8% g/mL-solvent) significantly reduce its carbon economy. In terms of the environmental footprints, PT is the most sustainable process followed by RCF and CTH. It is important to note that RCF pulps are not considered as utilizable products in Fig. 9, due to limited use of RCF pulps in the literature. Nonetheless, when RCF pulps are included in the calculation,
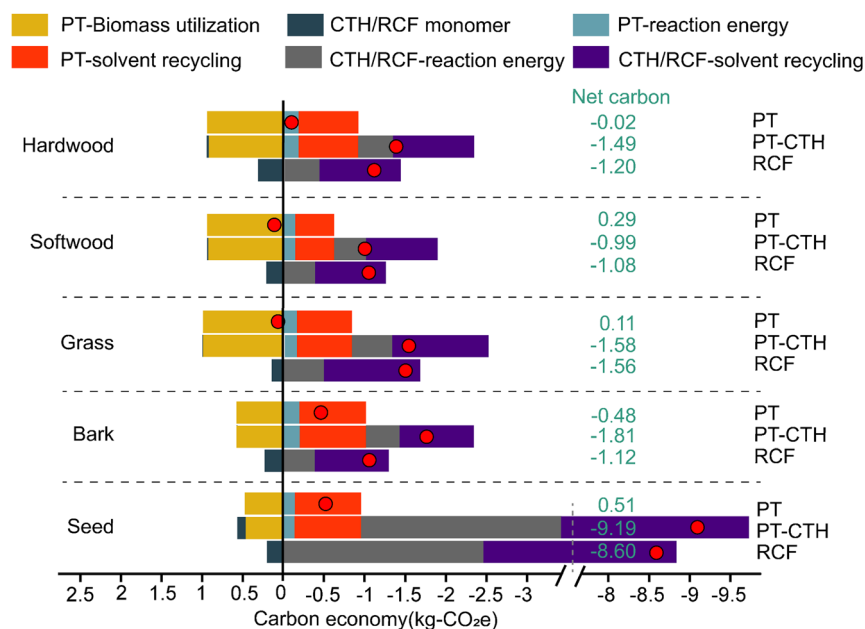

Fig. 9 Carbon economy (in $kg-CO_2e$) comparison between PT-CTH and RCF.

Table 5 *E*-Factor calculation

For 1 kg biomass	Utilizable products (kg)				By-products (kg)			Solvent waste (kg)		Catalyst waste (kg)		Enzyme waste (kg)		*E*-Factor				
	PT	CTH	RCF	RCF (+pulp)	PT	CTH	RCF	PT	CTH/RCF	CTH	RCF	PT	CTH/RCF	PT	CTH	PT-CTH	RCF	RCF (+pulp)
Hardwood	0.56	0.016	0.18	0.76	0.12	0.135	0.21	0.37	0.66	0.005	0.004	0.007	—	0.88	50.69	1.98	4.91	1.14
Softwood	0.56	0.007	0.12	0.87	0.19	0.184	0.26	0.24	0.55	0.005	0.005	0.007	—	0.77	106.91	1.73	6.74	0.93
Grass	0.59	0.005	0.08	0.68	0.12	0.142	0.31	0.34	0.74	0.005	0.005	0.007	—	0.79	188.46	2.04	12.99	1.55
Barks	0.34	0.006	0.14	0.57	0.21	0.142	0.51	0.41	0.57	0.005	0.004	0.005	—	1.81	123.79	3.42	8.04	1.92
Seed coats	0.28	0.070	0.11	0.77	0.35	0.077	0.67	0.41	3.91	0.010	0.010	0.003	—	2.68	57.03	13.08	39.86	5.93

Table 6 Cost–benefit analysis

For 1 kg biomass	Monomer (US$)		Oligomer (US$)		Ethanol (US$)	Pulp (US$)		Catalyst waste (US$)		Solvent waste (US$)		Enzyme waste (US$)		Revenue-cost (US$)				
	PT-CTH	RCF	PT-CTH	RCF	PT	CTH	RCF	CTH	RCF	PT	CTH/RCF	PT	CTH/RCF	PT	CTH	PT-CTH	RCF	RCF (+pulp)
Hardwood	$0.254	$1.507	—	$0.157	$0.181	—	$0.275	$0.376	$0.325	$0.110	$0.304	$0.030	—	$0.041	−$0.425	−$0.385	$1.035	$1.309
Softwood	$0.112	$0.713	—	$0.144	$0.180	—	$0.355	$0.180	$0.364	$0.071	$0.254	$0.031	—	$0.077	−$0.518	−$0.441	$0.239	$0.594
Grass	$0.076	$0.729	—	$0.068	$0.188	—	$0.281	$0.188	$0.346	$0.102	$0.342	$0.030	—	$0.056	−$0.642	−$0.586	$0.108	$0.389
Barks	$0.094	$1.215	—	$0.113	$0.110	—	$0.203	$0.110	$0.334	$0.122	$0.265	$0.020	—	−$0.033	−$0.547	−$0.579	$0.730	$0.933
Seed coats	$1.134	$0.988	—	$0.102	$0.090	—	$0.311	$0.090	$0.715	$0.122	$1.811	$0.011	—	−$0.043	−$1.450	−$1.493	−$1.436	−$1.126

both PT and RCF have similar net carbon, with PT being slightly higher (Table S10). These findings highlight three important recommendations, i.e., increase the solid loading, explore the possibility of utilizing RCF pulps, and increase the monomer yield in CTH.

4.5.2. E-Factor. E-Factor is the preliminary quantitative measure of environmental factors, defined as waste divided by utilizable products.[145] The wastes include by-product solvent waste, catalyst waste, and enzyme waste; while utilizable products are monomers, oligomers, and carbohydrate recovered. The E-factors of PT, PT-CTH, and RCF of various biomass feedstocks were calculated and are shown in Table 5. The most favorable feedstocks for PT-CTH and RCF are softwood and hardwood, respectively. However, when RCF pulps are included in the calculation, softwood becomes the best feedstock for RCF. In terms of the process, PT has lowest the E-factor, followed by RCF and CTH. Under the assumption of 96% solvent recycling, solvent waste contributes to approximately 75% of total waste. These findings emphasize the importance of complete solvent recovery in the biorefinery.

4.5.3. Cost–benefit analysis. Cost–benefit analysis was performed by calculating the profitability of each process. Revenues are generated from the sale of monomers, oligomers, ethanol, and pulp. Costs include catalyst, solvent, and enzyme wasted during the process. Table 6 compares the profitability between PT, PT-CTH, and RCF. Prices of raw materials and products were taken from various literature studies.[146,148,156,173–176] Three important assumptions must be emphasized here, i.e., the monomer price is equal to the vanillin price (16.2 US$ per kg),[173] the catalyst price is equal to the Pt/C catalyst price estimated by Baddour et al. (NREL),[176] and the catalyst recycling rate is 96%. In this case, RCF is more profitable than PT and CTH across all biomass species, due to the high contribution of monomer sale to the revenue. The best feedstock for both PT-CTH and RCF is hardwood. However, when the monomer price drops to 1.89 US$ per kg (the price in a techno-economic study by Liao et al.),[156] the

contribution of ethanol and pulp to the revenue increases, resulting in similar profitability between hardwood and softwood for both PT-CTH and RCF (with pulp). In terms of the cost, the catalyst and solvent have similar contributions, emphasizing the need to decrease catalyst dosage and increase solid loading.

5. Recommendations and prospects

5.1. Recommendations

By combining the analysis in section 4, it is possible to recommend the best biomass for each process and vice versa, the best process for each biomass. The criteria for deciding the recommendation are biomass potential, monomer yield and selectivity, environmental factors, and economic feasibility. Tables 7 and 8 demonstrate the recommendation for each biomass and for each process. Overall, RCF is the recommended process among most biomass feedstocks and hardwood is the recommended biomass for most processes. For maximizing monomer and economic factors, RCF of hardwood is recommended. In terms of environmental factors, PT of softwood is recommended. It can be observed that PT-CTH is not recommended in all biomass species, but PT-CTH can fully harness biomass potential. To achieve this, more optimization needs to be performed in future research, with the aim to increase the monomer yield of PT-CTH to a comparable value to that of RCF.

Several recommendations for future research, which apply to all biomass species and all processes, can be proposed:

1. Improve the monomer yield of PT-CTH through usage of a protection agent during pretreatment or catalytic cleaving of the C–C bond.

2. Increase the solid loading to reduce solvent usage.

3. Reduce the catalyst dosage to increase profitability.

4. Find effective ways to utilize RCF pulps, such as for hydrolysis to sugars and cellulose-based material production.

Table 7 Recommended process for each biomass

Biomass	Process	Biomass potential	Monomer	Environmental sustainability	Economic feasibility	Best process for this biomass
Hardwood	PT			x		RCF
	PT-CTH	x				
	RCF		x		x	
Softwood	PT	x		x		PT/RCF
	PT-CTH					
	RCF		x		x	
Grass	PT			x		RCF
	PT-CTH	x				
	RCF		x		x	
Barks	PT	x		x		PT/RCF
	PT-CTH					
	RCF		x		x	
Seed coats	PT			x		RCF
	PT-CTH		x			
	RCF	x			x	
Best process for this criterion		PT-CTH	RCF	PT	RCF	

Table 8 Recommended biomass for each process

Process	Biomass	Biomass potential	Monomer	Environmental sustainability	Economic feasibility	Best biomass for this process
PT	Hardwood					Softwood
	Softwood	x		x	x	
	Grass					
	Barks					
	Seed coats					
PT-CTH	Hardwood	x			x	Hardwood
	Softwood			x		
	Grass					
	Barks					
	Seed coats		x			
RCF	Hardwood		x	x	x	Hardwood
	Softwood			x		
	Grass					
	Barks					
	Seed coats	x				
RCF (+pulp)	Hardwood	x	x		x	Hardwood
	Softwood			x		
	Grass					
	Barks					
	Seed coats					
Best biomass for this criterion	Hardwood		Hardwood/seed coats	Softwood	Hardwood	

5. Completely recover the solvent and catalyst to minimize waste and costs.

5.2. Methods to improve the monomer yield of PT-CTH

5.2.1. Protection agent to preserve β-O-4 and/or prevent C–C condensation in PT-CTH. Since the monomer yield is mostly affected by the innate β-O-4/benzodioxane content, it is difficult to gauge the effect of pretreatment by direct comparison of monomer yields across different types of biomass feedstocks. Therefore, monomer yields were normalized against theoretical RCF yields, with these yields set as 100% normalized monomer yield for each biomass type. After normalization, Ouyang et al.'s study showed that as delignification increased from 44% to 77%, the normalized monomer yield decreased from 75% to 49%, primarily due to the cleavage of β-O-4 followed by lignin condensation facilitated by stable C–C bond formation during pretreatment.[99] Meanwhile, Shuai's study compared conditions with and without formaldehyde protection under similar delignification levels (∼70%). In this case, the normalized monomer yield was around 91% with formaldehyde protection, compared to approximately 47% without it.[26] From the HSQC NMR results, it was noted that formaldehyde was able to protect the β-O-4 bond. Usage of formaldehyde[44] and propionaldehyde[167] during pretreatment of spruce resulted in a CTH monomer yield of 20.56% and 20.10% g/g-lignin respectively.

Another study utilized *p*-toluene sulfonic acid to encapsulate dissolved lignin and prevent C–C condensation. The study found that although the β-O-4 content decreases from 57.8% to 36.1% after pretreatment, the monomer yield only decreases from 41% (RCF) to 30% g/g-lignin. Therefore, it was hypothesized that instead of preservation of β-O-4, the prevention of C–C condensation after β-O-4 cleavage is more crucial to obtain a high monomer yield.[23] Overall, these findings suggest that incorporation of protective agents in PT-CTH can preserve β-O-4 and/or prevent C–C condensation, thereby achieving potential monomer recoveries close to theoretical limit obtained in RCF.

5.2.2. Catalytical cleaving of C–C bonds. In general, C–O interunit bonds have lower bond dissociation energy (BDE) compared to C–C linkages, and the most abundant linkage in lignin from all natural sources is the β-O-4 linkage (C–O bond). In native lignin, C–O bonds take up around 2/3rd of all linkages between monomers and the rest are all C–C linkages. However, for technical lignin that is often attained from the industrial pulping process and for the lignin obtained from PT-CTH process, the substitution of ether bonds for recalcitrant C–C bonds (lignin condensation) is prevalent within its structure.[177] Therefore, an effective method to cleave the C–C bond will be beneficial for improving the monomer yield of lignin depolymerization in PT-CTH.

For the C–C bonds in lignin, the reaction pathways of its reductive cleavage were rarely investigated previously. There are two major oxidative routes for the scission of the Cα–Cβ bond that had been reported before *i.e.*, oxidation of Cβ to peroxide after the formation of Cα ketone, and direct abstraction of Cβ–H from the photocatalyst to form free radicals.[178,179] Although the modification of Cβ–H is the rate-determining step in both pathways, the direct activation without transformation into a ketone intermediate was only viable through photocatalysis, namely the photo-induced hole generation on the catalyst. Regarding the C–C bond cleavage in CTH, one of the proposed mechanisms is the retro-aldol pathway for the breakage of Cα–Cβ in β-O-4 model compounds, which requires hydrogen abstraction from Cγ–OH to form a Cγ aldehyde intermediate.

Finally, it is important to note that the CTH process was predominantly studied *via* the experiments with lignin model compounds in previous research, yet the mechanistic differ-
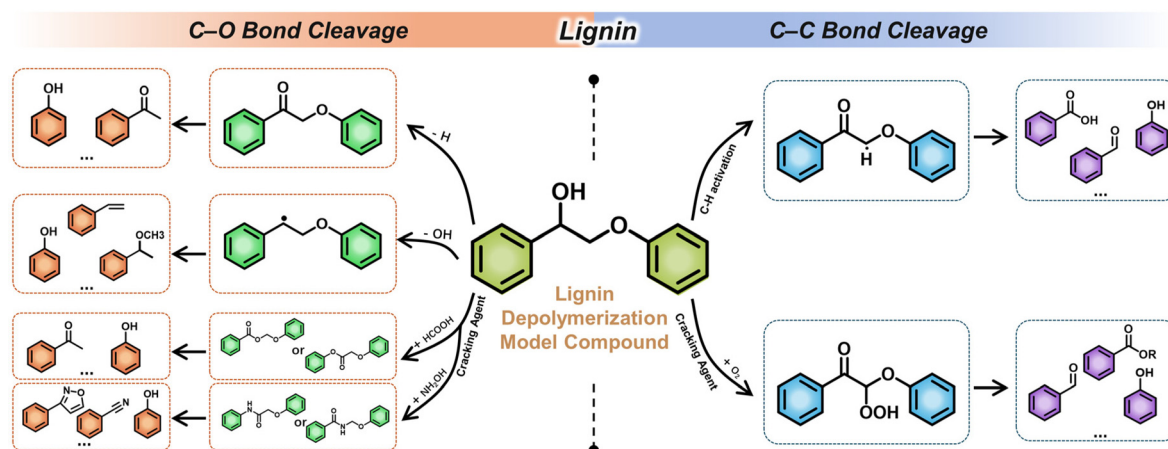
Fig. 10 Mechanism and final products of catalytical cleavage of the C−O bond and the C−C bond in lignin.

ence between CTH with model compounds and real lignin needs to be further elucidated in the future. In terms of cleavage pathways of different lignin interunit linkages, C–O bonds, especially the β-O-4 linkages, have been extensively studied. Meanwhile for the cleavage of C–C bonds, most studies focus on oxidative approaches rather than hydrogenolysis. In recent years, there are more discoveries on the self-hydrogen transfer mechanism in studies on CTH, which is in line with the general trend of developing green chemical processes. Fig. 10 summarizes the mechanism of C–O and C–C cleavage in lignin.

5.3. Modern setup of RCF

In industrial settings, majority of the production costs in RCF is attributed to the catalyst and the solvent. The RCF setup which can facilitate recycling of the catalyst and solvent can significantly reduce production cost in the industry. Anderson *et al.* (2017) designed a flowthrough multi-bed RCF reactor in 2017 that substituted a conventional batch reactor.[139] While catalyst deactivation and product repolymerization occurred rapidly during the operation of their device, catalyst recycling is more amenable, and the multi-bed design enabled in-depth analysis for reaction intermediates. In a batch reactor, possible methods to recycle the catalyst without sacrificing the monomer yield include the usage of magnetic catalysts such as RuO_x/γ-Fe_2O_3 [145] and the porous catalyst basket.[141] On the other hand, recycling of lignin oil can be done to lower solvent consumption and reduce downstream cost while maintaining a high monomer yield, but at the cost of 71–85% reduction in cellulose retention when the reaction is conducted in solvents with a high lignin concentration of 60–100% wt%.[180]

Since hydrogen gas is inherently dangerous and explosive, attempts to replace hydrogen with safer gases have been made. Atmospheric reductive catalytic fractionation (ARCF) is operated in an open vessel without hydrogen, which can improve the cost-effectiveness and safety of the process. While the monomer yield of ARCF was significantly lower than *via* a conventional route, the product selectivity towards oxidized mono-

mers increased.[9] Experiments conducted in a hydrogen-free environment revealed that a comparable monomer yield can be attained in hydrogen-free RCF of poplar when using the catalysts Pd/C and Pt/C (25–30% g/g-lignin in both cases with/without H_2), but a lower yield was observed with Ru/C and Ni/C. However, high selectivity towards propanol-G/S in Pd/C and Pt/C catalysts was only observed when 30 bar H_2 was used, while in a hydrogen-free environment, high ethyl-G/S is observed in Pd/C and high propylene-G/S is observed with Pt/C. Meanwhile, selectivity towards propyl-G/S in Ru/C and Ni/C remains high with/without hydrogen.[181] Also, RCF conducted in an N_2 environment resulted in a comparable monomer yield (35.8% g/g-lignin under N_2 *vs.* 46.0% g/g-lignin under H_2 in birch; 17.3% g/g-lignin under N_2 *vs.* 22.6% g/g-lignin under H_2 in wheat straw) with different target monomers (propenyl-side chain monomers under N_2 *vs.* propyl-side chain monomers under H_2 with the Ru/C catalyst).[130,151]

In summary, the RCF process has been extensively investigated from the aspects of process setup, solvent effects, catalyst effects, gas effects, recycling, and product separation. Most research studies focus on the lignin depolymerization stage when implementing mechanistic analysis, while delineations of how lignin–carbohydrate (LC) linkages change during RCF are rarely reported. The predominantly used setup for RCF requires the direct supply of hydrogen, but efficient RCFs with hydrogen-donating solvents and new catalysts have been increasingly covered in recent studies, which might bring changes to the state-of-the-art process design in the future.

5.4. Future directions

Based on the extensive discussion in this study, the summary and future research directions are listed in Fig. 11. It is important to note that this study has three limitations *i.e.*, it only includes PT-CTH with acid-based organosolv and acid-based DES pretreatment, the relative value of the monomer yield of seed coats is expressed in g/g-C-lignin based on the ^{13}C NMR results which is not a widely accepted method yet, and some assumptions were made in the data analysis and calculations
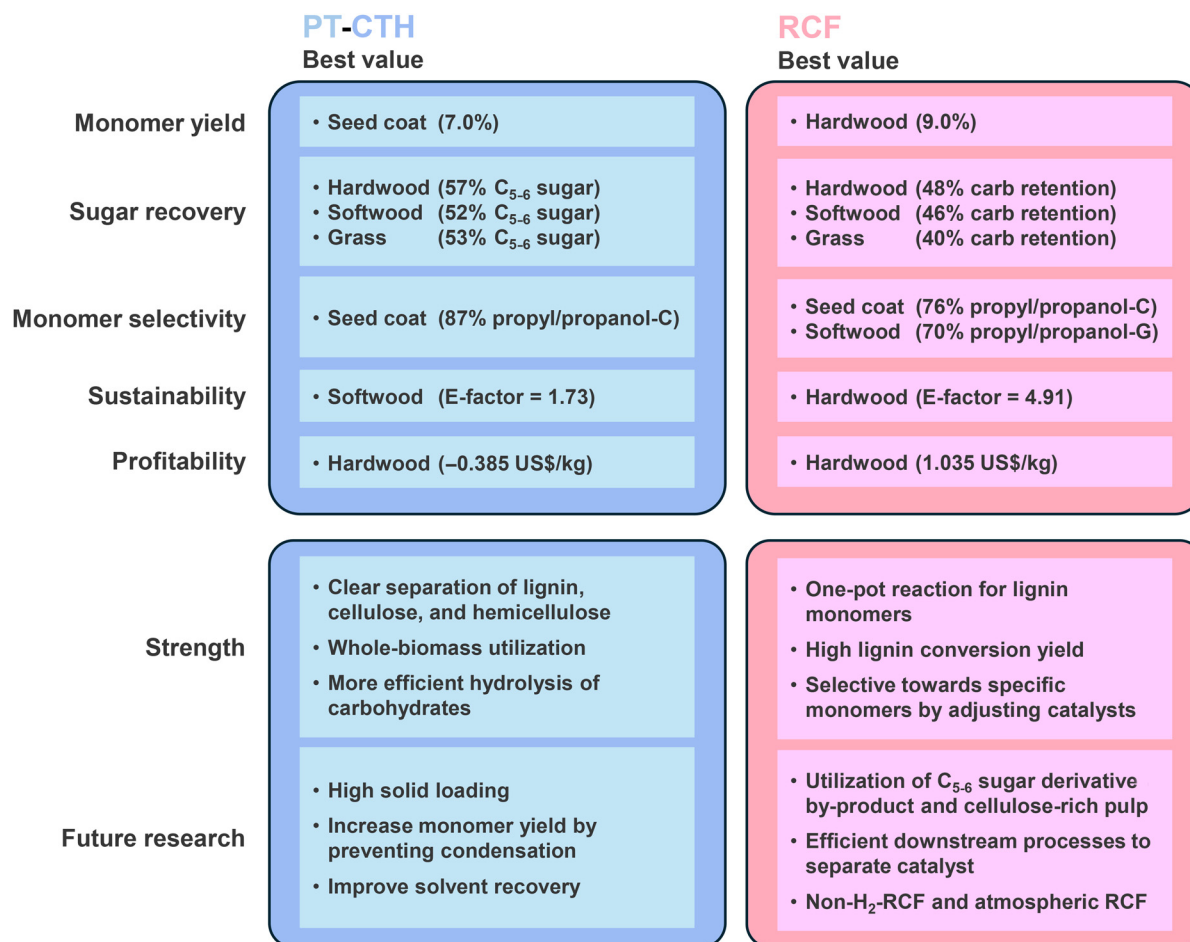
Fig. 11 Summary and future research directions.

such as prediction of the PT-CTH monomer yield with (β-O-4 content)[2].[101] In addition to the future works mentioned in Fig. 11, other research directions can be considered *i.e.*, faster preliminary analysis of the β-O-4 content to predict the monomer yield, catalytic cleaving of the C–C bond, lignin oil recycling, and analysis methods to accurately determine lignin in barks and seed coats.

6. Conclusion

This study provides a comprehensive insight into two thermochemical conversion processes (RCF and PT-CTH) of five biomass types, *i.e.*, hardwood, softwood, grass, barks, and seed coats. Overall, RCF produces higher monomer yield with hardwood being the best biomass, while PT-CTH produces higher utilizable products particularly C_{5-6} sugar derivatives from cellulose and hemicellulose. Hardwood, softwood, and grass produce higher utilizable products in PT-CTH and potentially usable products in RCF due to higher contents of carbohydrates. Seed coats, enriched with acid-resistant C-lignin, exhibit high potential for efficient aromatic monomer production *via* PT-CTH and RCF, but demonstrate low resource utilization. Barks are the

only biomass which can produce both phenolic and aliphatic monomers. The choice of solvents and protective agents during pretreatment plays a crucial role in minimizing condensation of lignin and thus increasing the monomer yield. In both RCF and CTH processes, strong correlations were observed between catalyst choice (Ru-based or Pd-based) and monomer selectivity. These findings offer specific processing recommendations for each biomass type, advancing sustainable biorefinery operations that maximize value recovery and economic profitability from diverse lignocellulosic feedstocks. The insights gained here support the development of green biorefinery systems towards optimized whole-biomass utilization.

Conflicts of interest

There are no conflicts to declare.

Data availability

The data supporting this article have been included as part of the SI. The SI contains all the experimental data collected from

the literature with cited references, as well as the calculated data and corresponding data analysis methods. See DOI: https://doi.org/10.1039/d5gc02627j.

Acknowledgements

References

1 R. J. Khan, C. Y. Lau, J. Guan, C. H. Lam, J. Zhao, Y. Ji, H. Wang, J. Xu, D.-J. Lee and S.-Y. Leu, *Bioresour. Technol.*, 2022, **346**, 126419.

2 T. Li, C. Chen, A. H. Brozena, J. Zhu, L. Xu, C. Driemeier, J. Dai, O. J. Rojas, A. Isogai and L. Wågberg, *Nature*, 2021, **590**, 47–56.

3 M. K. Islam, A. Thaemngoen, C. Y. Lau, J. Guan, C. S. Yeung, S. Chaiprapat and S.-Y. Leu, *Bioresour. Technol.*, 2021, **326**, 124766.

4 C. Zhao, Z. Hu, L. Shi, C. Wang, F. Yue, S. Li, H. Zhang and F. Lu, *Green Chem.*, 2020, **22**, 7366–7375.

5 N. Singh, R. R. Singhania, P. S. Nigam, C.-D. Dong, A. K. Patel and M. Puri, *Bioresour. Technol.*, 2022, **344**, 126415.

6 K. Robak and M. Balcerek, *Microbiol. Res.*, 2020, **240**, 126534.

7 S. Wang, G. Dai, H. Yang and Z. Luo, *Prog. Energy Combust. Sci.*, 2017, **62**, 33–86.

8 H. Li, A. Bunrit, N. Li and F. Wang, *Chem. Soc. Rev.*, 2020, **49**, 3748–3763.

9 T. Ren, S. You, Z. Zhang, Y. Wang, W. Qi, R. Su and Z. He, *Green Chem.*, 2021, **23**, 1648–1657.

10 M. M. Abu-Omar, K. Barta, G. T. Beckham, J. S. Luterbacher, J. Ralph, R. Rinaldi, Y. Román-Leshkov, J. S. Samec, B. F. Sels and F. Wang, *Energy Environ. Sci.*, 2021, **14**, 262–292.

11 A. J. Ragauskas, G. T. Beckham, M. J. Biddy, R. Chandra, F. Chen, M. F. Davis, B. H. Davison, R. A. Dixon, P. Gilna and M. Keller, *science*, 2014, **344**, 1246843.

12 X. Ouyang, X. Huang, B. M. S. Hendriks, M. D. Boot and E. J. M. Hensen, *Green Chem.*, 2018, **20**, 2308–2319.

13 T. Renders, G. Van den Bossche, T. Vangeel, K. Van Aelst and B. Sels, *Curr. Opin. Biotechnol.*, 2019, **56**, 193–201.

14 X. Liu, S. Feng, Q. Fang, Z. Jiang and C. Hu, *Mol. Catal.*, 2020, **495**, 111164.

15 M. Chen, Y. Li, F. Lu, J. S. Luterbacher and J. Ralph, *ACS Sustainable Chem. Eng.*, 2023, **11**, 10001–10017.

16 J. H. Jang, A. R. C. Morais, M. Browning, D. G. Brandner, J. K. Kenny, L. M. Stanley, R. M. Happs, A. S. Kovvali, J. I. Cutler, Y. Román-Leshkov, J. R. Bielenberg and G. T. Beckham, *Green Chem.*, 2023, **25**, 3660–3670.

17 S. Su, L.-P. Xiao, X. Chen, S. Wang, X.-H. Chen, Y. Guo and S.-R. Zhai, *ChemSusChem*, 2022, **15**, e202200365.

18 T. Zhang, R. Kumar and C. E. Wyman, *Carbohydr. Polym.*, 2013, **92**, 334–344.

19 J. M. Pepper and H. Hibbert, *J. Am. Chem. Soc.*, 1948, **70**, 67–71.

20 Z. Wang, S. Winestrand, T. Gillgren and L. J. Jönsson, *Biomass Bioenergy*, 2018, **109**, 125–134.

21 J. M. Pepper and R. W. Fleming, *Can. J. Chem.*, 1978, **56**, 896–898.

22 N. Li, Y. Li, C. G. Yoo, X. Yang, X. Lin, J. Ralph and X. Pan, *Green Chem.*, 2018, **20**, 4224–4235.

23 Z. Wang, S. Qiu, K. Hirth, J. Cheng, J. Wen, N. Li, Y. Fang, X. Pan and J. Y. Zhu, *ACS Sustainable Chem. Eng.*, 2019, **7**, 10808–10820.

24 L. Chen, J. Dou, Q. Ma, N. Li, R. Wu, H. Bian, D. J. Yelle, T. Vuorinen, S. Fu, X. Pan and J. Zhu, *Sci. Adv.*, 2017, **3**, e1701735.

25 T. Renders, E. Cooreman, S. Van den Bosch, W. Schutyser, S. F. Koelewijn, T. Vangeel, A. Deneyer, G. Van den Bossche, C. M. Courtin and B. F. Sels, *Green Chem.*, 2018, **20**, 4607–4619.

26 L. Shuai, M. T. Amiri, Y. M. Questell-Santiago, F. Héroguel, Y. Li, H. Kim, R. Meilan, C. Chapple, J. Ralph and J. S. Luterbacher, *Science*, 2016, **354**, 329–333.

27 T. Vangeel, T. Renders, K. Van Aelst, E. Cooreman, S. Van den Bosch, G. Van den Bossche, S.-F. Koelewijn, C. Courtin and B. Sels, *Green Chem.*, 2019, **21**, 5841–5851.

28 K. Van Aelst, E. Van Sinay, T. Vangeel, E. Cooreman, G. Van den Bossche, T. Renders, J. Van Aelst, S. Van den Bosch and B. F. Sels, *Chem. Sci.*, 2020, **11**, 11498–11508.

29 J.-X. Wang, S. Asano, S. Kudo and J.-I. Hayashi, *ACS Omega*, 2020, **5**, 29168–29176.

30 Y. Yamashita, C. Sasaki and Y. Nakamura, *J. Biosci. Bioeng.*, 2010, **110**, 79–86.

31 D. Warren-Walker, S. R. Ravella, J. Gallagher, A. Winters, A. Charlton and D. N. Bryant, *Bioresour. Technol.*, 2024, **405**, 130932.

32 Z. Jiang, B. Fei and Z. Li, *Bioresour. Technol.*, 2016, **214**, 876–880.

33 J. Sun, R. Ding and J. Yin, *Biochem. Eng. J.*, 2022, **177**, 108270.

34 S. P. Joy and C. Krishnan, *Ind. Crops Prod.*, 2022, **177**, 114409.

35 J. Zeng, G. L. Helms, X. Gao and S. Chen, *J. Agric. Food Chem.*, 2013, **61**, 10848–10857.

36 F. Brienza, K. Van Aelst, F. Devred, D. Magnin, B. F. Sels, P. A. Gerin, I. Cybulska and D. P. Debecker, *ACS Sustainable Chem. Eng.*, 2022, **10**, 11130–11142.

37 Q. Zheng, T. Zhou, Y. Wang, X. Cao, S. Wu, M. Zhao, H. Wang, M. Xu, B. Zheng, J. Zheng and X. Guan, *Sci. Rep.*, 2018, **8**, 1321.

38 M. Usia and S. Kara, *Holz Roh- Werkst.*, 1997, **55**, 268–268.

39 M. Balaban Ucar and G. Uçar, *Holzforschung*, 2001, **55**, 478–486.

40 J. Samec, S. Muangmeesri, D. Lebedeva, L. Ramazanova, S. Liu, H. Khalili, A. P. Mathew and J. Ralph, *Oxidative Valorization of Spruce Bark to Yield Vanillin*, 2024.

41 R. Khan, G. Jianyu, C. Lau, H. Zhuang, S. Rehman and S.-Y. Leu, *ChemSusChem*, 2024, **17**, e202301306.

42 W.-Z. Yin, S.-L. Zou, L.-P. Xiao and R.-C. Sun, *Chem. Eng. Sci.*, 2024, **288**, 119828.

43 M. L. Stone, E. M. Anderson, K. M. Meek, M. Reed, R. Katahira, F. Chen, R. A. Dixon, G. T. Beckham and Y. Román-Leshkov, *ACS Sustainable Chem. Eng.*, 2018, **6**, 11211–11218.

44 Y. Li, L. Shuai, H. Kim, A. H. Motagamwala, J. K. Mobley, F. Yue, Y. Tobimatsu, D. Havkin-Frenkel, F. Chen, R. A. Dixon, J. S. Luterbacher, J. A. Dumesic and J. Ralph, *Sci. Adv.*, 2018, **4**, eaau2968.

45 S. Wang, K. Zhang, H. Li, L.-P. Xiao and G. Song, *Nat. Commun.*, 2021, **12**, 416.

46 W. Xia, C. Cui, L. Shao, Y. Liu, X. Li, C. Wang, D. Zhao and F. Xu, *Sep. Purif. Technol.*, 2025, **353**, 128487.

47 S. Su, Q. Shen, S. Wang and G. Song, *Int. J. Biol. Macromol.*, 2023, **239**, 124256.

48 S. Su, S. Wang and G. Song, *Green Chem.*, 2021, **23**, 7235–7242.

49 H. G. Ahn, J. E. Lee, H. Kim, H. J. Jung, K. K. Oh, S. H. Heo and J. S. Kim, *Polysaccharides*, 2024, **5**, 552–566.

50 X. Cheng, R. Ning, F. Zhang, L. Ji, K. Wang and J. Jiang, *Biomass Bioenergy*, 2023, **170**, 106708.

51 J. Lupoi, S. Singh, R. Parthasarathi, B. Simmons and R. Henry, *Renewable Sustainable Energy Rev.*, 2015, **49**, 871–906.

52 C. G. Yoo, A. Dumitrache, W. Muchero, J. Natzke, H. Akinosho, M. Li, R. W. Sykes, S. D. Brown, B. Davison, G. A. Tuskan, Y. Pu and A. J. Ragauskas, *ACS Sustainable Chem. Eng.*, 2018, **6**, 2162–2168.

53 L. Ana and P. Helena, in *Lignin*, ed. P. Matheus, IntechOpen, Rijeka, 2017, ch. 3, DOI: 10.5772/intechopen.71208.

54 G. van Erven, N. Nayan, A. S. Sonnenberg, W. H. Hendriks, J. W. Cone and M. A. Kabel, *Biotechnol. Biofuels*, 2018, **11**, 1–16.

55 G. van Erven, V. J. Boerkamp, J. W. van Groenestijn and R. J. Gosselink, *Green Chem.*, 2024, **26**, 7101–7112.

56 B. Ai, W. Li, J. Woomer, M. Li, Y. Pu, Z. Sheng, L. Zheng, A. Adedeji, A. J. Ragauskas and J. Shi, *Green Chem.*, 2020, **22**, 6372–6383.

57 H. Kim, D. Padmakshan, Y. Li, J. Rencoret, R. D. Hatfield and J. Ralph, *Biomacromolecules*, 2017, **18**, 4184–4195.

58 M. Tahoun, C. T. Gee, V. E. McCoy, M. Stoneman, V. Raicu, M. Engeser and C. E. Müller, *Sci. Rep.*, 2024, **14**, 118.

59 A. Ježo, *J. Renewable Mater.*, 2024, **12**, 1029–1042.

60 F. Chen, Y. Tobimatsu, D. Havkin-Frenkel, R. A. Dixon and J. Ralph, *Proc. Natl. Acad. Sci. U. S. A.*, 2012, **109**, 1772–1777.

61 Y. Wang, S. Su and G. Song, *Polymers*, 2023, **15**, 2732.

62 P. Wang, S. Wang, S. Su, D. Zhang, Y. Liao, G. Song and L. Wang, *Green Chem.*, 2025, **27**, 3207–3216.

63 M. M. Abu-Omar, K. Barta, G. T. Beckham, J. S. Luterbacher, J. Ralph, R. Rinaldi, Y. Román-Leshkov, J. S. M. Samec, B. F. Sels and F. Wang, *Energy Environ. Sci.*, 2021, **14**, 262–292.

64 A. D. Sluiter, B. R. Hames, R. O. Ruiz, C. J. Scarlata, J. Sluiter, D. W. Templeton and D. P. Crocker, *Determination of Structural Carbohydrates and Lignin in Biomass*, NREL, 2004.

65 T. Vangeel, T. Renders, K. Van Aelst, E. Cooreman, S. Van den Bosch, G. Van den Bossche, S. F. Koelewijn, C. M. Courtin and B. F. Sels, *Green Chem.*, 2019, **21**, 5841–5851.

66 S. Feng, S. Cheng, Z. Yuan, M. Leitch and C. Xu, *Renewable Sustainable Energy Rev.*, 2013, **26**, 560–578.

67 Y. Su, T. Feng, C.-B. Liu, H. Huang, Y.-L. Wang, X. Fu, M.-L. Han, X. Zhang, X. Huang, J.-C. Wu, T. Song, H. Shen, X. Yang, L. Xu, S. Lü and D.-Y. Chao, *Nat. Plants*, 2023, **9**, 1968–1977.

68 J. Zhang, C. Zhang, X. Li, Z.-Y. Liu, X. Liu and C.-L. Wang, *Plant Mol. Biol.*, 2023, **112**, 341–356.

69 A. E. Harman-Ware, S. Sparks, B. Addison and U. C. Kalluri, *Biotechnol. Biofuels*, 2021, **14**, 75.

70 Y. Ao, Q. Wu, J. Zheng, C. Zhang, Y. Zhao, R. Xu, K. Xue, C. Dai and M. Yang, *Plant Sci.*, 2024, 112300, DOI: 10.1016/j.plantsci.2024.112300.

71 C. Liu, S. Wang, B. Wang and G. Song, *Ind. Crops Prod.*, 2021, **169**, 113666.

72 S. Wang, S. Su, L.-P. Xiao, B. Wang, R.-C. Sun and G. Song, *ACS Sustainable Chem. Eng.*, 2020, **8**, 7031–7038.

73 S.-Y. Leu and J. Y. Zhu, *Bioenergy Res.*, 2013, **6**, 405–415.

74 X. Zhao, S. Li, R. Wu and D. Liu, *Biofuels, Bioprod. Biorefin.*, 2017, **11**, 567–590.

75 M. Kuglarz, M. Alvarado-Morales, K. Dąbkowska and I. Angelidaki, *Bioresour. Technol.*, 2018, **265**, 191–199.

76 S.-Y. Leu, J. Zhu, R. Gleisner, J. Sessions and G. Marrs, *Biomass Bioenergy*, 2013, **59**, 393–401.

77 M. K. Islam, S. Rehman, J. Guan, C.-Y. Lau, H.-Y. Tse, C. S. Yeung and S.-Y. Leu, *Appl. Energy*, 2021, **303**, 117653.

78 C. M. Martínez, D. A. Cantero and M. J. Cocero, *J. Cleaner Prod.*, 2018, **204**, 888–895.

79 J. Fernández-Rodríguez, X. Erdocia, F. Hernández-Ramos, M. G. Alriols and J. Labidi, in *Separation of Functional Molecules in Food by Membrane Technology*, ed. C. M. Galanakis, Academic Press, 2019, pp. 229–265. DOI: 10.1016/B978-0-12-815056-6.00007-3.

80 J. S. Kim, Y. Y. Lee and T. H. Kim, *Bioresour. Technol.*, 2016, **199**, 42–48.

81 R. S. Abolore, S. Jaiswal and A. K. Jaiswal, *Carbohydr. Polym. Technol. Appl.*, 2024, **7**, 100396.

82 J. Zhang, W. Zhang, Z. Cai, J. Zhang, D. Guan, D. Ji and W. Gao, *ACS Omega*, 2022, **7**, 18761–18769.

83 X. Xu, K. Wang, Y. Zhou, C. Lai, D. Zhang, C. Xia and A. Pugazhendhi, *Fuel*, 2023, **338**, 127361.

84 S. Han, R. Wang, K. Wang, J. Jiang and J. Xu, *Bioresour. Technol.*, 2022, **363**, 127905.

85 Z.-M. Zhao, X. Meng, B. Scheidemantle, Y. Pu, Z.-H. Liu, B.-Z. Li, C. E. Wyman, C. M. Cai and A. J. Ragauskas, *Bioresour. Technol.*, 2022, **347**, 126367.

86 C. Dong, X. Meng, C. S. Yeung, H.-Y. Tse, A. J. Ragauskas and S.-Y. Leu, *Green Chem.*, 2019, **21**, 2788–2800.

87 H. Qin, X. Hu, J. Wang, H. Cheng, L. Chen and Z. Qi, *Green Energy Environ.*, 2020, **5**, 8–21.

88 L. Das, M. Li, J. Stevens, W. Li, Y. Pu, A. J. Ragauskas and J. Shi, *ACS Sustainable Chem. Eng.*, 2018, **6**, 10408–10420.

89 B. B. Hansen, S. Spittle, B. Chen, D. Poe, Y. Zhang, J. M. Klein, A. Horton, L. Adhikari, T. Zelovich, B. W. Doherty, B. Gurkan, E. J. Maginn, A. Ragauskas, M. Dadmun, T. A. Zawodzinski, G. A. Baker, M. E. Tuckerman, R. F. Savinell and J. R. Sangoro, *Chem. Rev.*, 2021, **121**, 1232–1285.

90 M. Zhang, R. Tian, H. Han, K. Wu, B. Wang, Y. Liu, Y. Zhu, H. Lu and B. Liang, *J. Cleaner Prod.*, 2022, **345**, 131028.

91 Z. Sun, B. Fridrich, A. de Santi, S. Elangovan and K. Barta, *Chem. Rev.*, 2018, **118**, 614–678.

92 H. Yang, C. G. Yoo, X. Meng, Y. Pu, W. Muchero, G. A. Tuskan, T. J. Tschaplinski, A. J. Ragauskas and L. Yao, *Bioresour. Technol.*, 2020, **295**, 122240.

93 C. Cai, N. Li, H. Liu, J. Zhang, J. Zhu and F. Wang, *Chem. Eng. J.*, 2023, **453**, 139730.

94 M. K. Islam, J. Guan, S. Rehman, R. D. Patria, C. Hu, L. Guan, S.-Y. Leu and A. K. Vuppaladadiyam, *Biomass Convers. Biorefin.*, 2024, **14**, 5435–5446.

95 C. G. Yoo, M. Li, X. Meng, Y. Pu and A. J. Ragauskas, *Green Chem.*, 2017, **19**, 2006–2016.

96 C. Dong, X. Meng, S.-Y. Leu, L. Xu, Z. Wu, G. Cravotto and Z. Fang, *Ind. Crops Prod.*, 2022, **185**, 115130.

97 Z. Wang, S. Qiu, K. Hirth, J. Cheng, J. Wen, N. Li, Y. Fang, X. Pan and J. Zhu, *ACS Sustainable Chem. Eng.*, 2019, **7**, 10808–10820.

98 W. Lan, M. T. Amiri, C. M. Hunston and J. S. Luterbacher, *Angew. Chem., Int. Ed.*, 2018, **57**, 1356–1360.

99 X. Ouyang, X. Huang, B. M. Hendriks, M. D. Boot and E. J. Hensen, *Green Chem.*, 2018, **20**, 2308–2319.

100 J. Bär, T. Phongpreecha, S. K. Singh, M. Kral Yilmaz, C. E. Foster, J. D. Crowe and D. B. Hodge, *Biomass Convers. Biorefin.*, 2018, **8**, 813–824.

101 T. Phongpreecha, N. C. Hool, R. J. Stoklosa, A. S. Klett, C. E. Foster, A. Bhalla, D. Holmes, M. C. Thies and D. B. Hodge, *Green Chem.*, 2017, **19**, 5131–5143.

102 C. Huang, Y. Zhan, J. Wang, J. Cheng, X. Meng, L. Liang, F. Liang, Y. Deng, G. Fang and A. J. Ragauskas, *Green Chem.*, 2022, **24**, 3736–3749.

103 A. Hideno, A. Kawashima, T. Endo, K. Honda and M. Morita, *Bioresour. Technol.*, 2013, **132**, 64–70.

104 L. Matsakas, V. Raghavendran, O. Yakimenko, G. Persson, E. Olsson, U. Rova, L. Olsson and P. Christakopoulos, *Bioresour. Technol.*, 2019, **273**, 521–528.

105 P. Sannigrahi, S. J. Miller and A. J. Ragauskas, *Carbohydr. Res.*, 2010, **345**, 965–970.

106 L. Wang, M. Min, Y. Li, P. Chen, Y. Chen, Y. Liu, Y. Wang and R. Ruan, *Appl. Biochem. Biotechnol.*, 2010, **162**, 1174–1186.

107 L. Xu, J. Zhang, Q.-J. Zong, L. Wang, T. Xu, J. Gong, Z.-H. Liu, B.-Z. Li and Y.-J. Yuan, *Chem. Eng. J.*, 2022, **427**, 130962.

108 Y. Kim, A. Yu, M. Han, G. W. Choi and B. Chung, *J. Chem. Technol. Biotechnol.*, 2010, **85**, 1494–1498.

109 P. Obama, G. Ricochon, L. Muniglia and N. Brosse, *Bioresour. Technol.*, 2012, **112**, 156–163.

110 C. Vanderghem, Y. Brostaux, N. Jacquet, C. Blecker and M. Paquot, *Ind. Crops Prod.*, 2012, **35**, 280–286.

111 G. Yu, B. Li, C. Liu, Y. Zhang, H. Wang and X. Mu, *Ind. Crops Prod.*, 2013, **50**, 750–757.

112 J. Wildschut, A. T. Smit, J. H. Reith and W. J. Huijgen, *Bioresour. Technol.*, 2013, **135**, 58–66.

113 U. Jomnonkhaow, S. Sittijunda and A. Reungsang, *Renewable Energy*, 2022, **181**, 1237–1249.

114 L.-Y. Liu, S. C. Patankar, R. P. Chandra, N. Sathitsuksanoh, J. N. Saddler and S. Renneckar, *ACS Sustainable Chem. Eng.*, 2020, **8**, 4745–4754.

115 B. Rietzler, M. Karlsson, I. Kwan, M. Lawoko and M. Ek, *Biomacromolecules*, 2022, **23**, 3349–3358.

116 A. Romaní, A. Larramendi, R. Yáñez, Á. Cancela, Á. Sánchez, J. A. Teixeira and L. Domingues, *Ind. Crops Prod.*, 2019, **132**, 327–335.

117 K. Hrůzová, L. Matsakas, U. Rova and P. Christakopoulos, *Bioresour. Technol.*, 2021, **341**, 125855.

118 M. Pals, M. Lauberts, D. S. Zijlstra, J. Ponomarenko, A. Arshanitsa and P. J. Deuss, *Molecules*, 2022, **27**, 3185.

119 W. Lan, M. T. Amiri, C. M. Hunston and J. S. Luterbacher, *Angew. Chem.*, 2018, **130**, 1434–1434.

120 Y. Bai, X.-F. Zhang, Z. Wang, T. Zheng and J. Yao, *Bioresour. Technol.*, 2022, **347**, 126723.

121 Y. Liu, N. Deak, Z. Wang, H. Yu, L. Hameleers, E. Jurak, P. J. Deuss and K. Barta, *Nat. Commun.*, 2021, **12**, 5424.

122 Q. Yu, A. Zhang, W. Wang, L. Chen, R. Bai, X. Zhuang, Q. Wang, Z. Wang and Z. Yuan, *Bioresour. Technol.*, 2018, **247**, 705–710.

123 T. Suopajärvi, P. Ricci, V. Karvonen, G. Ottolina and H. Liimatainen, *Ind. Crops Prod.*, 2020, **145**, 111956.

124 X. Zhou, X. Zeng, S. Hu, Y. Zhou, M. Xie and F. Yue, *Chem. Eng. J.*, 2024, **497**, 154340.

125 Q. Zhai, F. Long, X. Jiang, C.-Y. Hse, J. Jiang and J. Xu, *Ind. Crops Prod.*, 2020, **158**, 113018.

126 K. Nie, S. Liu, T. Zhao, Z. Tan, Y. Zhang, Y. Song, B. Li, L. Li, W. Lv, G. Han and W. Jiang, *Biomass Convers. Biorefin.*, 2022, **14**, 28755–28765.

127 G. Shen, X. Yuan, Y. Cheng, S. Chen, Z. Xu and M. Jin, *Green Chem.*, 2023, **25**, 8026–8039.

128 Z. Liu, H. Li, X. Gao, X. Guo, S. Wang, Y. Fang and G. Song, *Nat. Commun.*, 2022, **13**, 4716.

129 M. Jindal, P. Uniyal and B. Thallada, *Bioresour. Technol.*, 2023, **385**, 129396.

130 H. Huang, X. Zhang, L. Ma and Y. Liao, *Angew. Chem., Int. Ed.* e202502545.

131 I. Klein, B. Saha and M. M. Abu-Omar, *Catal. Sci. Technol.*, 2015, **5**, 3242–3245.

132 E. Sheridan, S. Filonenko, A. Volikov, J. A. Sirviö and M. Antonietti, *Green Chem.*, 2024, **26**, 2967–2984.

133 R. Rinken, D. Posthuma and R. Rinaldi, *ChemSusChem*, 2023, **16**, e202201875.

134 M. Jindal, A. Kumar, S. Rawat and B. Thallada, *Sustainable Energy Fuels*, 2023, **7**, 3926–3938.

135 Q. Wang, L.-P. Xiao, Y.-H. Lv, W.-Z. Yin, C.-J. Hou and R.-C. Sun, *ACS Catal.*, 2022, **12**, 11899–11909.

136 X. Li, R. Ma, X. Gao, H. Li, S. Wang and G. Song, *Adv. Sci.*, 2024, **11**, 2310202.

137 E. M. Anderson, R. Katahira, M. Reed, M. G. Resch, E. M. Karp, G. T. Beckham and Y. Román-Leshkov, *ACS Sustainable Chem. Eng.*, 2016, **4**, 6940–6950.

138 Y. Li, Y. Yu, Y. Lou, S. Zeng, Y. Sun, Y. Liu and H. Yu, *Angew. Chem., Int. Ed.*, 2023, **62**, e202307116.

139 E. M. Anderson, M. L. Stone, R. Katahira, M. Reed, G. T. Beckham and Y. Román-Leshkov, *Joule*, 2017, **1**, 613–622.

140 J. K. Kenny, S. R. Neefe, D. G. Brandner, M. L. Stone, R. M. Happs, I. Kumaniaev, W. P. Mounfield III, A. E. Harman-Ware, K. M. Devos, T. H. I. V. Pendergast, J. W. Medlin, Y. Román-Leshkov and G. T. Beckham, *JACS Au*, 2024, **4**, 2173–2187.

141 S. Van den Bosch, T. Renders, S. Kennis, S. F. Koelewijn, G. Van den Bossche, T. Vangeel, A. Deneyer, D. Depuydt, C. M. Courtin, J. M. Thevelein, W. Schutyser and B. F. Sels, *Green Chem.*, 2017, **19**, 3313–3326.

142 S. Van den Bosch, W. Schutyser, R. Vanholme, T. Driessen, S. F. Koelewijn, T. Renders, B. De Meester, W. J. J. Huijgen, W. Dehaen, C. M. Courtin, B. Lagrain, W. Boerjan and B. F. Sels, *Energy Environ. Sci.*, 2015, **8**, 1748–1763.

143 W. Arts, K. Van Aelst, E. Cooreman, J. Van Aelst, S. Van den Bosch and B. F. Sels, *Energy Environ. Sci.*, 2023, **16**, 2518–2539.

144 Z. Zhang, C. W. Lahive, J. G. M. Winkelman, K. Barta and P. J. Deuss, *Green Chem.*, 2022, **24**, 3193–3207.

145 F. Bugli, A. Baldelli, S. Thomas, M. Sgarzi, M. Gigli, C. Crestini, F. Cavani and T. Tabanelli, *ACS Sustainable Chem. Eng.*, 2024, **12**, 16638–16651.

146 A. W. Bartling, M. L. Stone, R. J. Hanes, A. Bhatt, Y. Zhang, M. J. Biddy, R. Davis, J. S. Kruger, N. E. Thornburg, J. S. Luterbacher, R. Rinaldi, J. S. M. Samec, B. F. Sels, Y. Román-Leshkov and G. T. Beckham, *Energy Environ. Sci.*, 2021, **14**, 4147–4168.

147 X. Yang, J. Yu, M. Zeng, Z. Luo and H. Zhang, *J. Anal. Appl. Pyrolysis*, 2025, **188**, 107049.

148 M. Tschulkow, T. Compernolle, S. Van den Bosch, J. Van Aelst, I. Storms, M. Van Dael, G. Van den Bossche, B. Sels and S. Van Passel, *J. Cleaner Prod.*, 2020, **266**, 122022.

149 M. D. Garrett, S. C. Bennett, C. Hardacre, R. Patrick and G. N. Sheldrake, *RSC Adv.*, 2013, **3**, 21552–21557.

150 T. Nicolaï, W. Arts, S. Calderon-Ardila, R. Smets, M. Van Der Borght, J. M. Thevelein and B. F. Sels, *ACS Sustainable Chem. Eng.*, 2024, **12**, 8353–8365.

151 F. Brienza, K. Van Aelst, F. Devred, D. Magnin, B. F. Sels, P. Gerin, I. Cybulska and D. P. Debecker, *ChemSusChem*, 2023, **16**, e202300103.

152 D. Cao, J. Zhang, Y. Nie, S. Wang, X. Feng, J. Zhu, X. Lu and L. Mu, *Chem. Eng. Sci.*, 2023, **266**, 118288.

153 S. Muangmeesri, N. Li, D. Georgouvelas, P. Ouagne, V. Placet, A. P. Mathew and J. S. M. Samec, *ACS Sustainable Chem. Eng.*, 2021, **9**, 17207–17213.

154 S. Su, Q. Shen, S. Wang and G. Song, *Int. J. Biol. Macromol.*, 2023, **239**, 124256.

155 F. Jiang, W. Zheng, C. Zhang, B. Jiang, Z. Li, J. Cheng, Y. Zhang, B. Luo, X. Shen and Y. Jin, *Ind. Crops Prod.*, 2025, **228**, 120913.

156 Y. Liao, S. F. Koelewijn, G. Van den Bossche, J. Van Aelst, S. Van den Bosch, T. Renders, K. Navare, T. Nicolaï, K. Van Aelst, M. Maesen, H. Matsushima, J. M. Thevelein, K. Van Acker, B. Lagrain, D. Verboekend and B. F. Sels, *Science*, 2020, **367**, 1385–1390.

157 X. Liu, F. P. Bouxin, J. Fan, R. Gammons, V. L. Budarin, C. Hu and J. H. Clark, *Ind. Crops Prod.*, 2021, **167**, 113515.

158 D. G. Brandner, J. S. Kruger, N. E. Thornburg, G. G. Facas, J. K. Kenny, R. J. Dreiling, A. R. C. Morais, T. Renders, N. S. Cleveland, R. M. Happs, R. Katahira, T. B. Vinzant, D. G. Wilcox, Y. Román-Leshkov and G. T. Beckham, *Green Chem.*, 2021, **23**, 5437–5441.

159 M. Hou, H. Chen, Y. Li, H. Wang, L. Zhang and Y. Bi, *Energy Fuels*, 2022, **36**, 1929–1938.

160 T. Renders, W. Schutyser, S. V. D. Bosch, S.-F. Koelewijn, T. Vangeel, C. M. Courtin and B. F. Sels, *ACS Catal.*, 2016, **6**, 2055–2066.

161 P. Ferrini and R. Rinaldi, *Angew. Chem., Int. Ed.*, 2014, **53**, 8634–8639.

162 Z. Dou, Z. Zhang and M. Wang, *Appl. Catal., B*, 2022, **301**, 120767.

163 X. Gong, J. Sun, X. Xu, B. Wang, H. Li and F. Peng, *Bioresour. Technol.*, 2021, **333**, 124977.

164 H. Guo, B. Zhang, Z. Qi, C. Li, J. Ji, T. Dai, A. Wang and T. Zhang, *ChemSusChem*, 2017, **10**, 523–532.

165 A. Mabrouk, X. Erdocia, M. G. Alriols and J. Labidi, *J. Cleaner Prod.*, 2018, **198**, 133–142.

166 E. M. Anderson, M. L. Stone, R. Katahira, M. Reed, W. Muchero, K. J. Ramirez, G. T. Beckham and Y. Román-Leshkov, *Nat. Commun.*, 2019, **10**, 2033.

167 W. Lan, M. T. Amiri, C. M. Hunston and J. S. Luterbacher, *Angew. Chem., Int. Ed.*, 2018, **57**, 1356–1360.

168 C. Dong, X. Meng, C. S. Yeung, T. Ho-Yin, A. J. Ragauskas and S.-Y. Leu, *Green Chem.*, 2019, **21**, 2788–2800.

169 K. Zhang, H. Li, L.-P. Xiao, B. Wang, R.-C. Sun and G. Song, *Bioresour. Technol.*, 2019, **285**, 121335.

170 Q. Yu, A. Zhang, W. Wang, L. Chen, R. Bai, X. Zhuang, Q. Wang, Z. Wang and Z. Yuan, *Bioresour. Technol.*, 2018, **247**, 705–710.

171 A. T. Smit, M. Hoek, P. A. Bonouvrie, A. van Zomeren, L. A. Riddell and P. C. Bruijnincx, *ACS Sustainable Chem. Eng.*, 2024, **12**, 4731–4742.

172 L. Krotz and G. Giazzi, *Elemental Analysis: CHNS/O characterization of biomass and bio-fuels*, Thermo Fisher Scientific, 2017.

173 A. J. Robinson, A. Giuliano, O. Y. Abdelaziz, C. P. Hulteberg, A. Koutinas, K. S. Triantafyllidis, D. Barletta and I. De Bari, *Bioresour. Technol.*, 2022, **364**, 128004.

174 D. Humbird, R. Davis, L. Tao, C. Kinchin, D. Hsu and A. Aden, *Process Design and Economics for Biochemical Conversion of Lignocellulosic Biomass to Ethanol*, NREL, 2011.

175 J.-L. Zheng, Y.-H. Zhu, H.-Y. Su, G.-T. Sun, F.-R. Kang and M.-Q. Zhu, *Renewable Sustainable Energy Rev.*, 2022, **167**, 112714.

176 F. G. Baddour, L. Snowden-Swan, J. D. Super and K. M. Van Allsburg, *Org. Process Res. Dev.*, 2018, **22**, 1599–1605.

177 S. Guadix-Montero and M. Sankar, *Top. Catal.*, 2018, **61**, 183–198.

178 T. Hou, N. Luo, H. Li, M. Heggen, J. Lu, Y. Wang and F. Wang, *ACS Catal.*, 2017, **7**, 3850–3859.

179 C. Zhang and F. Wang, *Acc. Chem. Res.*, 2020, **53**, 470–484.

180 J. H. Jang, J. Callejón Álvarez, Q. S. Neuendorf, Y. Román-Leshkov and G. T. Beckham, *ACS Sustainable Chem. Eng.*, 2024, **12**, 12919–12926.

181 J. K. Kenny, D. G. Brandner, S. R. Neefe, W. E. Michener, Y. Román-Leshkov, G. T. Beckham and J. W. Medlin, *React. Chem. Eng.*, 2022, **7**, 2527–2533.